Geoderma 461 (2025) 117452

Contents lists available at ScienceDirect

Geoderma

journal homepage: www.elsevier.com/locate/geoderma

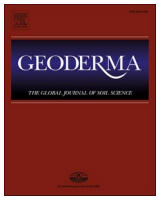

Drivers of soil organic carbon stocks and stability along elevation gradients

Nicolas Bonfanti [a,b,*], Philippe Choler [c], Norine Khedim [a], Jean-Christophe Clément [b], Pierre Barré [d], Romain Goury [c], François Baudin [e], Lauric Cécillon [d,f], Amélie Saillard [c], Wilfried Thuiller [c], Jerome Poulenard [a], THE ORCHAMP Consortium

[a] Univ. Savoie Mont Blanc, CNRS, EDYTEM, Chambéry, France
[b] Univ. Savoie Mont Blanc, INRAE, CARRTEL, Thonon-Les-Bains, France
[c] Univ. Grenoble Alpes, Univ. Savoie Mont Blanc, CNRS, LECA F-38000 Grenoble, France
[d] Laboratoire de Géologie, École Normale Supérieure, CNRS, PSL University, IPSL, Paris, France
[e] Sorbonne Université, CNRS, ISTeP 75005 Paris, France
[f] French Embassy, Nairoby, Kenya

ARTICLE INFO

Handling Editor: Dr Cornelia Rumpel

Keywords:
Rock-Eval® analysis
Soil organic matter
Mountain ecosystems
Pedosequences
Soil weathering
Climate stabilization

ABSTRACT

Estimating SOC stocks and stability, as well as modeling their response to rising temperatures, is crucial for predicting climate change impacts. This is particularly true in mountainous regions, where low temperatures slow down SOC decomposition, resulting in higher SOC stocks compared to soils at lower elevations. However, these stocks are also more vulnerable to warming, increasing the risk of SOC depletion. Such conditions create the potential for a positive feedback loop in which warming accelerates SOC losses, further amplifying climate change impacts on these sensitive ecosystems.

To better understand the factors controlling SOC stocks and stability in mountain soils, we sampled 170 soil profiles along 29 elevation gradients in the western Alps from 280 to 3160 m a.s.l. We assessed SOC stocks and chemical composition using mid-infrared spectroscopy method and SOC stability with Rock-Eval® thermal analysis. Our findings, based on an unprecedented dataset, reveal a clear elevational pattern in SOC properties. SOC stocks increase with elevation up to the montane belt (1200–1500 m a.s.l.), remain relatively stable through the subalpine zone, and then decline beyond the subalpine/alpine boundary (2200–2400 m a.s.l.). Notably, this transition is also marked by a significant drop in SOC stability, suggesting a shift in the dominant stabilization processes at higher elevations. Our results also indicate that SOC stocks and stability are influenced by a complex interplay of factors.

At higher elevations, climate emerges to be the dominant factor, whereas lithology and weathering play a more significant role at lower elevations. These results suggest that at high-elevations, harsh climatic conditions favor stabilization of SOC, while less developed soils limit organo-mineral interactions. In contrast, at warmer, lower elevations with higher carbon fluxes, more developed soils facilitate organo-mineral interactions, thereby enhancing SOC stability in the long term. Consequently, alpine grasslands, which contain substantial stocks of labile carbon stabilized by climatic conditions, appear to be particularly vulnerable to the effects of climate warming.

1. Introduction

1.1. Key role of soil organic carbon

Soils store two to three times more carbon than the atmosphere, with global soil organic carbon (SOC) stocks estimated at around 1500–2400 Gt C (Batjes, 1996; Jobbagy and Jackson, 2000). This large SOC reservoir is contained in soil organic matter (SOM), raising concerns about its evolution with ongoing climate change (Trumbore and Czimczik, 2008; Wiesmeier et al., 2019). Understanding SOM dynamics and feedback mechanisms with warming is essential for improving climate models and for understanding ecosystem functioning (Crowther et al., 2016). While quantification of SOC stocks is necessary, it is not sufficient to assess their vulnerability to climate change. The three main

* Corresponding author.
E-mail address: nicolas.bonfanti.usmb@gmail.com (N. Bonfanti).

https://doi.org/10.1016/j.geoderma.2025.117452
Received 18 February 2025; Received in revised form 30 April 2025; Accepted 21 July 2025
Available online 2 August 2025

mechanisms governing SOM stability (or persistence) – chemical recalcitrance, organo-mineral interactions (O-M interactions), and climate stabilization – must also be considered (Fig. 1.B; Amelung et al., 2008; Kögel-Knabner et al., 2008; Lorenz et al., 2007; Schmidt et al., 2011).

1.2. SOC vulnerability to climate change in mountain ecosystems

Mountain regions, such as the Alps, are particularly vulnerable to climate change due to their specific environmental conditions and accurately estimating SOC stocks in these areas remains challenging because of their high spatial variability (climatic, lithologic or biologic gradients) (Trumbore, 1993; Wiesmeier et al., 2014). Cold ecosystems, including alpine and polar regions, have higher SOC stocks than temperate ecosystems due to low temperatures that limit mineralization and result in organic matter accumulation (Davidson and Janssens, 2006; Leifeld et al., 2009; Schadt et al., 2003). In alpine environments, SOC seems primarily stabilized by low temperatures, while O-M interactions and chemical recalcitrance play a lesser role in these young soils where the stabilization of labile molecules is facilitated by cold conditions. As a result, SOC stocks in these regions are both large and labile (i.e., with low stability), making them particularly vulnerable to climate change (Leifeld et al., 2005). The subsequent release of greenhouse gases (i.e., CO_2, CH_4) from these soils could create positive feedback loops and amplify global warming (Bonfanti et al., 2025b; Dorrepaal et al., 2009; Prietzel et al., 2016).

Field measurements in mountainous regions are sporadic due to difficult access. In addition, mountain soils typically contain high levels of coarse elements due in particular to gravitational processes (e.g., debris, moraines) and to the early stage of pedogenesis, which limits SOC storage (Garcia-Pausas et al., 2007; Leifeld et al., 2005) and leads to overestimation of SOC stocks (Poeplau et al., 2017). Therefore, a more comprehensive understanding of the spatial structure of SOC stocks and their stability in mountainous environments is critical for anticipating the consequences of climate change, especially as these regions will experience more pronounced warming than lowland areas (EEA, E.E.A., 2024; Pepin et al., 2015).

1.3. Drivers of SOC properties

SOC properties, including stocks and stability, are shaped by a combination of factors that drive soil genesis, collectively referred to as "CLORPT": climate, organisms (plant and microbial activity), relief (topography), parent material (bedrock) and time (soil age and weathering state) (Fig. 1.B; Duchaufour et al., 2024; Jenny, 1947; Legros, 2007):

- Soil climate influences both temperature and hydrological regimes, which regulate mineral weathering, biological activity, O-M interactions, and carbon fluxes.
- Topography further modifies soil climate through slope and exposure, while also affecting particle fluxes, such as erosion and deposition, which are critical for SOC dynamics (Fig. 1.B, links 1, 2, 6, 7).
- Bedrock lithology plays a pivotal role in determining soil properties, including pH, mineral composition, grain size, and weathering conditions. These properties influence SOC stabilization through O-M interactions and biological processes.
- Soil age influences SOC characteristics not only by determining the duration of organic matter inputs (Khedim et al., 2022), but also by shaping the soil's weathering stage, which in turn affects grain size distribution, mineralogy, pH, organo-mineral interactions, and biological activity (Fig. 1.B, links 3, 4, 10, 11, 12, 13).

Biological activity, driven by soil communities and vegetation type, regulates the input and decomposition of organic matter. Different ecosystems, such as grasslands and forests, contribute differently to SOC turnover. Vegetation also influences litter quality—characterized by stoichiometry (C/N ratios) and chemical composition (recalcitrance)—which in turn shapes SOC mineralization rates (Fig. 1.B, links 5, 8, 9).

1.4. Contribution of CLORPT factors in mountain soils

The relative contribution of CLORPT factors is complex to estimate and varies in different environments and studies. Studies shows that climate influences SOC storage primarily through its indirect effects on vegetation and soil properties (Benayas et al., 2004). However, other studies suggested that SOC variability in mountainous regions is more closely related to (meso-)topography than to vegetation (Burke et al., 1999; Egli et al., 2009). To analyze the interplay of these factors, elevation gradients are frequently used, providing insights into how SOC properties change with elevation (Yang et al., 2018). Some studies on elevation gradients have reported an increase in labile carbon content with elevation (Bonfanti et al., 2025d; Budge et al., 2011; Leifeld et al., 2009); however, this relationship varies depending on the elevation range and the specific study, indicating strong site dependence (Bangroo et al., 2017; Bojko and Kabala, 2017; Djukic et al., 2010; Garcia-Pausas et al., 2007).

Although the effects of climatic gradients on vegetation are well-studied (Choler, 2005; Körner, 2003), gaps remain in understanding how climate affects SOC quantity and stability (Canedoli et al., 2020). Elevation gradients often correspond to climatic, ecological, and vegetative stratification, which generally results in pedological gradients (pedosequences) due to changes in soil formation processes. In mountainous regions, pedosequences developed on carbonated (limestone, dolomite) and siliceous parent materials are commonly used to illustrate how pedogenetic processes—such as soil weathering (Egli et al., 2006)—and soil types (Dambrine, 1985; Egli and Poulenard, 2016) vary with elevation. These pedosequences provide a framework for analyzing SOC properties in relation to pedogenesis (Fig. 1.A).

1.5. Objectives and hypothesis

Understanding soil organic carbon (SOC) dynamics in mountain ecosystems is challenging due to the interplay of multiple environmental factors. To address this issue, this study examines SOC properties (stocks and stability) on an unprecedented dataset comprising 29 elevation gradients (170 plots) in the western Alps, spanning diverse temperature regimes, bedrock types, vegetation covers, and elevations (280 to 3160 m a.s.l.). We focus on grasslands and forests to identify key controls on SOC along elevation gradients. Our approach combines: (1) A pedogenetic analysis on SOC distribution along soil formation sequences (Fig. 1.A) and (2) a mechanistic assessment of CLORPT parameters to disentangle their relative influence on SOC properties (Fig. 1.B). By integrating descriptive and mechanistic perspectives, we aim to enhance understanding of SOC stabilization mechanisms and improve predictions of SOC vulnerability to climate change.

Specifically, we seek to identify the key parameters controlling SOC stocks and to assess their vulnerability to climate change, specifically focusing on soils with substantial labile SOC stocks stabilized by low temperatures. We hypothesize that:

(i) SOC stocks tend to increase with elevation due to the accumulation of labile organic matter, reaching a peak in the subalpine and alpine belts. Beyond this point, SOC stocks decline as productivity decreases at higher elevations;
(ii) SOC biogeochemical stability —driven by O-M interactions and chemical recalcitrance— declines at higher elevations as climate-driven stabilization becomes more dominant;
(iii) Climate primarily influences SOC properties in surface horizons, while lithology exerts a greater influence at depth. In highland areas, climate is the dominant control, whereas lithological

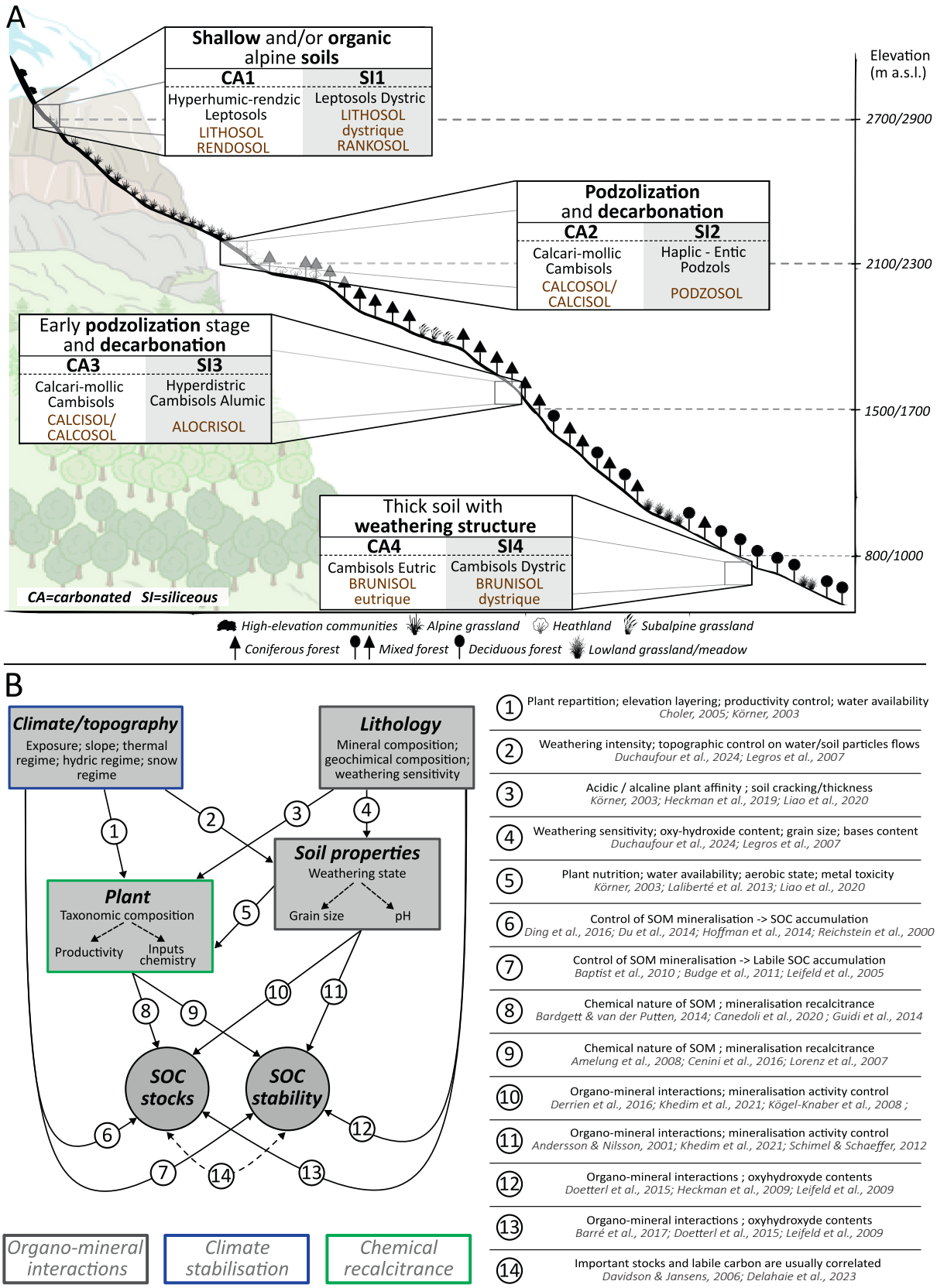

Fig. 1. Conceptual framework of the analysis. (A) The pedological approach illustrates classical pedosequences along an elevation gradient on both siliceous and carbonated rock. These pedosequences emerge as a result of variations in weathering, plant communities, and subsequent pedogenesis across elevations (Egli and Poulenard, 2016). Each study plot was associated with a specific position on these pedosequences (see Table S2 for detailed linkages). (B) The conceptual model of SOC stock and stability controls. Exogenous variables such as topography, climate and lithology influence both pedogenesis and plant distribution, which in turn affect SOC stocks and stability. This framework was used to perform structural equation modeling.

influences vary along the elevation gradient with a decrease of the control on O-M interactions with elevation.

2. Materials & methods

2.1. Study sites

We investigated SOC properties across 29 elevation gradients in the western Alps (Fig. 2, Table S1). The selected sites are part of the ORCHAMP observatory (Thuiller et al., 2024). Each gradient consists of 4 to 8 permanent plots at 200-meter elevation intervals, totaling 170 plots. These plots encompass the lithological, climatic, and biological diversity of the western Alps (Fig. 2, Table S1). The study plots, ranging from 280 to 3 160 m a.s.l., cover various parent rock types and are influenced by different climatic regimes, including oceanic conditions in the north, Mediterranean influences in the south, moist pre-Alpine massifs, and drier internal massifs. Land cover types include major vegetation categories, including deciduous, coniferous, and mixed forests, heathlands (ericaceous), rocky grasslands, and species-rich grasslands (Fig. 2, Table S1). This dataset provides a representative overview of the diverse soil types and pedogenetic processes occurring across the Alps.

2.2. Soil analysis

2.2.1. Soil sampling and description

For each plot, soil type was classified according to the French soil reference system (AFES, 2008) and the FAO soil description (FAO et al., 2006; WRB, 2022). Soil sampling campaigns were conducted from August to October between 2016 and 2023. Soil pits (~1 m × 1 m) were excavated from the surface down to the parent material, and each morphological horizon was described and sampled for analysis (Fig. 2, see also Fig. S1). Three soil replicates of 100 cm^3 were collected to assess bulk density and coarse elements content. Additionally, approximately 500 g of soil was collected for analysis of soil properties, soil weathering, and SOC characterization. These samples were air-dried for 1–2 weeks, sieved to 2 mm and ground.

Soil descriptions and soil properties were used to assign profiles to soil reference classes. This classification enabled the association of profiles with locations in classic pedosequences when applicable (Fig. 1. A; see Table S2 for specific plots assignation).

2.2.2. Soil properties

To characterize the main soil properties controlling SOC dynamics, the following analyses were performed on 2 mm-sieved samples following NF ISO 11464 standard: **pH_{H2O}**, **pH_{KCl}** (NF ISO 10390 standard), cation exchange capacity cobaltihexammine (**CEC**, NF ISO 23470 standard), exchangeable Al, Ca, Fe, Mg, Mn, K, Na cobaltihexammine (ICP-AES, NF ISO 23470 standard), **P available** (Olsen method, NF ISO

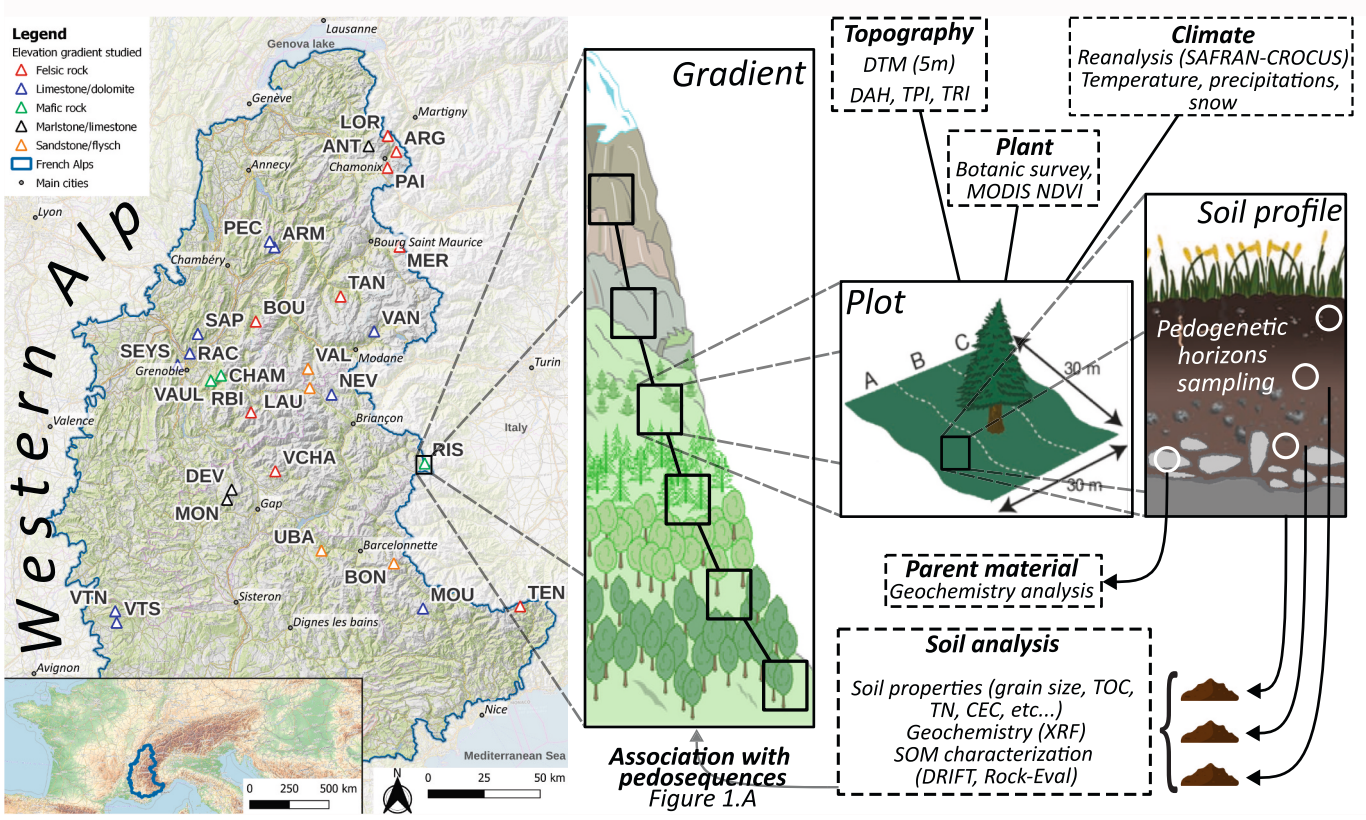

Fig. 2. Overall Analysis Methodology. Study sites are distributed throughout the French Alps across 29 elevation gradients. Each gradient includes four to nine study plots, spaced approximately 200 m apart in elevation. On these plots, we characterized topographic features (slope, aspect, DAH, TPI) using a 5-meter resolution digital terrain model. Climate variables were derived from the S2M SAFRAN CROCUS reanalysis model, providing long-term data (averaged on 1960–2020) on thermal and hydrological conditions, such as growing degree days, growing season length, total precipitation, and actual evapotranspiration. We assessed plant composition using a botanical pin-point survey and estimated plant productivity through MODIS NDVI remote sensing. Each plot's soil profile was analyzed through detailed description and sampling by pedogenetic horizons. Soil properties such as grain size, SOC characteristics and geochemistry were measured. These data allowed to classify soils according to the World Reference Base (WRB 2014) and the Référentiel Pédologique (RP2008), further linking soil profiles to their positions within pedosequences along the elevation gradient (refer to Fig. 1 and Table S2). Additionally, a sample of the bedrock was analyzed to determine its geochemical composition.

11263 standard), grain size distribution (**clay, silt, sand**; NF X 31–107 standard), carbonates ($\mathbf{CO_3}$), organic carbon content (**C**), total nitrogen (**TN**) (NF ISO 10693, NF ISO 10694, NF ISO 14235, NF ISO 13878 standards). **SOM** content was measured through loss on ignition (LOI) at 550 °C for 4 h. Delta pH ($\mathbf{\Delta_{pH}}$) was calculated as the difference between pH_{H2O} and pH_{KCl}. It provides insight into the difference between actual and potential acidity, reflecting the amount of H^+ ions adsorbed onto the CEC. High ΔpH values indicate that the CEC holds a substantial amount of exchangeable H^+ ions. In contrast, fertile soils typically exhibit low ΔpH values, suggesting lower levels of acidity and a higher base saturation.

2.2.3. SOC characterization

We used an analysis of SOM chemistry assessed by DRIFT analysis combined with a thermal analysis with RockEval® to characterized the SOC stability.

Soil samples were analyzed using diffuse reflectance infrared Fourier transform spectroscopy (DRIFT) with a Nicolet iS10 spectrometer (Thermo Fisher Scientific; Wadoux et al., 2021, see also Fig. S2.A for more details on methodology). Chemical functional group indices were calculated by integrating spectra over specific wavelength ranges, representing key carbon functional groups for characterizing the SOM chemistry (Bonfanti et al., 2025a; Khedim et al., 2021; Saenger et al., 2015): aliphatic index (3000 – 2750 cm^{-1}), carbonyl index (1750–1670 cm^{-1}) and aromatic index (1618 – 1576 cm^{-1}). Aliphatic index represents OM which require less activation energy and are more labile, while the aromatic and carbonyl indices characterize organic matter that is more resistant to mineralization. These indices were chosen because their spectral regions are minimally influenced by soil mineralogical composition (Soucémarianadin et al., 2019).

SOC stability was evaluated using Rock-Eval® 6 analysis (RE6) (Vinci Technologies, France) following the methodology of Cécillon et al., (2018) and Baudin (2023). Briefly, ~60 mg of finely ground soil sample was placed in an oven, and carbon gaseous effluents (CO, CO_2, HC) were analyzed in two phases. The pyrolysis phase involved a 3-minute isotherm at 200 °C, followed by a temperature ramp from 200 °C to 650 °C at a heating rate of 30 °C per minute in a nitrogen (N_2) atmosphere. The oxidation phase began with a 1-minute isotherm at 300 °C, followed by a temperature ramp from 300 °C to 850 °C at 20 °C per minute, with a 5-minute isotherm at 850 °C in a dried and CO_2-free laboratory air atmosphere. During this analysis, CO and CO_2 emissions were quantified using an infrared detector, while volatile hydrocarbon effluents (HC) are measured with a flame ionization detector.

Total organic carbon (TOC_RE6) was calculated as the sum of carbon fractions released during pyrolysis and oxidation, excluding inorganic carbon. SOC stability indices included the Hydrogen Index (**HI**), Oxygen Index (**OI**), the Pyrolysable Carbon to Total Organic Carbon ratio (**PC_TOC**), and temperature at which xx% of yy carbon forms (HC, CO or CO_2) is released during zz phase (oxidation or pyrolysis), summarized as **Txx_yy_zz** (for example, T50_CO2_PYR corresponds to the temperature at which 50 % of CO_2 was released during the pyrolysis phase). To interpret these indices, one must keep in mind that the higher the temperature, the more stable the SOC. For details on Rock-Eval® analysis principles and its application to SOM analysis, see Fig. S2 and Barré et al. (2023, 2016); Disnar et al. (2003); Sebag et al. (2016). For all abbreviations correspondence see Table S6.

2.3. CLORPT analysis

To assess the relative contribution of key environmental factors in controlling SOC properties, we characterized climate, land cover, parent material, and soil weathering (CLORPT) at each sampling plot.

2.3.1. Climate and topography analysis (CLTP)

Climatic and topographic (relief) data were analyzed together (CLTP), as local climate conditions are partly influenced by topography. Topographic variables were derived from a 5-meter resolution digital terrain model (IGN, 2001). Extracted indices included **aspect** (degrees relative to the south, from 0° = south to 180° = north), topographical position index (**TPI**: negative for depressions, positive for ridges, and close to zero for flat areas) (De Reu et al., 2013), and diurnal anisotropic heating (**DAH**), which quantifies solar radiation intensity based on slope and aspect (−1 = low intensity; 1 = high intensity). Topographic analysis were conducted using the "sf" (Pebesma et al., 2023), "terra" (Hijmans et al., 2023a), and "raster" (Hijmans et al., 2023b) R packages (R Core Team, 2023).

Climatic data were obtained from the S2M-SAFRAN-CROCUS climate reanalysis model for the French Alps (Durand et al., 2009; Vernay et al., 2022; Vionnet et al., 2012) and averaged from 1959 to 2020. We analyzed annual climate variables, including mean maximum and minimum daily temperatures (**Tmax** and **Tmin**, respectively, in °C), growing degree days (**GDD**, in °C), which measure heat accumulation as the annual sum of mean daily temperatures above 1 °C, precipitation water equivalent (**Prec**, in mm, combining rainfall and snowfall), maximum snow height (**Snow**), actual evapotranspiration (**ETP**, in mm), and water deficit (i.e., the balance between Rainfall and evapotranspiration, **DEF** = Rainfall-ETP, in mm).

Phenology was assessed via MODIS NDVI remote sensing (MOD09Q1 Terra Collection 6; 250 m resolution, 8 days composites) following Choler (2023). We determined growing season length (**GSL**, in days), snow season length (**SSL**, in days), and first snow-free day (**FSFD**, in Julian day) averaged from 2000 to 2020. Bioclimatic belts (collinean: 0–800 m a.s.l.; montane: 800–1500 m a.s.l.; subalpine: 1500–2200 m a.s.l.; alpine: 2200–2800 m a.s.l.; nival: 2800–3160 m a.s.l.) and slope orientation (north, east, south, west) were included as categorical variables.

2.3.2. Parent material analysis (LT = Lithology)

At each plot, a representative sample of the parent material was collected. The samples were crushed, quartered, and finely ground before being analyzed for elemental geochemical composition using X-ray fluorescence spectroscopy (S8 Tiger Series 2, Bruker, Towett et al., 2013). This analysis measured the relative proportion (%) of major elements (**CaO, MgO, K_2O, Na_2O, SiO_2, Al_2O_3, P_2O_5, MnO, TiO_2, Fe_2O_3**) and trace elements of parent material sample. Additionally, the geological context of the parent material was characterized using factorial information from the 1:50 000 geological map (BRGM, 2005, Table S1).

2.3.3. Plant analysis (VG = Vegetation)

Vegetation data were obtained through a combination of field surveys and remote sensing techniques. Plant species abundance was assessed by professional botanists during the peak growing and flowering season (July to August), using a pinpoint method adapted from Jonasson, (1988) (Thuiller et al., 2024). A 30-meter transect was laid perpendicular to the slope at the center of each plot. At 20 cm intervals along the transect, two observation points were established—one 25 cm upslope and the other 25 cm downslope. At each point, all plant species in contact were recorded. This approach resulted in a total of 300 measurements per plot, with each point potentially including multiple species.

Tree cover data were extracted from Copernicus TreeCover density (**treecover**) with a 100 m resolution (Copernicus, 2020). NDVI was calculated for each plot as a proxy for above-ground primary productivity. The annual time-integrated NDVI was computed using a threshold of 0.2, while NDVI amplitude was determined by the difference between its maximum and minimum values over the year. Factorial land cover information was extracted from the Corine Land Cover dataset (Copernicus, 2018), and validated through field observations. For modelling purposes, land cover types were aggregated into two broad categories: (i) forested habitats, encompassing all forest types, and (ii) non-forested habitats, including heathlands and grasslands.

2.3.4. Soil weathering (TRB)

The geochemical composition of each soil horizon was analyzed using X-ray fluorescence spectrometry, following the same protocol as for the parent material. From this data, a weathering index was calculated to quantify the loss of alterable elements in soils following Goldschmidt diagram (Brosens et al., 2021; Goldschmidt, 1930). To ensure consistency across different lithology, we adapted the **TRB** index, which sums the total positive charges of Ca, Mg, K, and Na in each sample, normalizing it to the TRB of the parent material (Equations 1, see Fig. S3 for the choice of weathering index). As mobile elements (Ca, K, Mg, Na) are leached through chemical weathering, TRB values decrease relative to the parent material. Notably, our TRB correction (Equations 1) is the inverse of conventional approach: the more weathered a soil, the higher its TRB, as the difference between elemental reserves in the bedrock and soil increases with weathering.

$$Equations1 \ : \ TRB_i = {Ca^{2+}}_i + {Mg^{2+}}_i + {K^{+}}_i + {Na^{+}}_i;$$

$$RelativeTRB_{H_x} = \frac{TRB_{LT} - TRB_{H_x}}{TRB_{LT}}$$

With: Ca_i^{2+}, Mg_i^{2+}, K_i^{+}, Na_i^{+} represent the charge equivalent of alkaline and alkaline-earth elements in sample i (soil horizon or parent material), and H_x = soil horizon x; LT = lithology under H_x horizon. TRB_{Hx} represents the total reserve of bases (TRB) in horizon x , while relative TRB_{Hx} refers to the TRB of horizon x normalized by the TRB of the underlying parent material, providing a corrected measure that accounts for the base status of the substrate beneath. Relative TRB_{Hx} is used to estimate soil weathering state.

3. Data correction

3.1. Fine soil stock correction

Since soil stock calculations are often overestimated due to improper accounting for coarse elements (Poeplau et al., 2017), we calculated fine soil stocks (S_{FS}) with the fine soil mass (m_{FS}) and coarse elements (m_{CCcyl}) within a 100 cm^3 cylinder (see Fig. S1 for the procedure of fine stock correction). The fine soil stock was then corrected based on the estimated volumetric proportion of coarse elements content (CC). Carbon stocks (**SOC_{stock}**, in kg/m^2 for the specified thickness) were then derived by multiplying fine soil stock by carbon content (%).

3.2. Systematic horizon conversion

Pedological horizon sampling provides a reliable and accurate characterization of soil properties within homogeneous morphological layers. However, depth variations between horizons complicate interplot comparisons. To standardized soil properties, we aggregated data into four fixed depth layers across all soil profiles: 0–10 cm, 0–30 cm, 30–50 cm, and the entire profile. This approach aligns with the methodology of Kanari et al. (2021), who demonstrated that Rock-Eval® characterization of an entire soil layer can be extrapolated from its sublayers. We extended this principle to other soil properties, assuming it holds across various parameters (Bishop et al., 1999; Hengl et al., 2017). Accordingly, variables were aggregated following Equation (2). This standardization was applied to all soil properties, including geochemical data (TRB was calculated *post hoc*), DRIFT parameters, and Rock-Eval® parameters. For parameters expressed as ratios (e.g., S/T; PC_TOC), both the numerator and denominator were corrected before recalculating the ratio.

$$Equation\,(2) : Property_{H_{sys}} = \sum_{\substack{Forall \\ Hi \cap H_{sys}}} Property_{H_i} * f_{H_i}$$

$$with : H_{sys} = systematichorizon(e.g. 0-10; 0-30; 30-50); H_i = morphologichorizoninH_{sys}; f_{H_i} = correctingfactor = \frac{S_{FS}ofH_i inH_{sys}}{totalS_{FS}inH_{sys}}$$

3.3. Statistical analysis

All data processing and analysis were performed using R software (R Core Team, 2023) and packages “reshape2”, “rstatix”, “dplyr” and “tidyverse” (Wickham et al., 2019). A first analysis was done along classical pedosequences, with morphological horizons as statistical individuals (Fig. 1.A), followed structural equation modelling (SEM) to assess and interpret a mechanistic approach (Fig. 1.B). For SEM mechanistic analysis, the statistical units were individual plots, each characterized by standardized depth intervals (i.e., systematic horizons of 0–30 cm or 30–50 cm). We also used coinertia analysis to test the mechanistic approach, results are available in supplementary materials (Figs. S5).

3.4. Regression and variance analysis

Factorial comparisons were performed across parent material lithology (crystalline, limestone, marlstone, moraine, ophiolite, sandstone), elevation belts (collinean, montane, subalpine, alpine and nival), land cover types (deciduous, mixed, coniferous forests, heathland, grassland and rocky grassland), and exposure (N, NO, NE, O, E, SO, SE and S). We used analysis of variance (ANOVA) to compare SOC stocks and stability (C.stab index; see below for details). To meet normality and homoscedasticity assumptions, data were log- or square-root transformed as needed. *Post hoc* pairwise comparisons were conducted using Tukey’s test ($p < 0.05$, adjusted for multiple comparisons). Variance partitioning assessed the contributions of SOC content, fine soil stock, and coarse element content to SOC stock across soil layers using the “vegan” package (Oksanen et al., 2022) and the “lme4” package (Bates et al., 2015) in R.

3.5. Multivariate analysis

To simplify the analysis, we have gathered explanatory variables into four groups: climate and topography (CLTP), lithology (LT), soil properties (SOIL) and vegetation (VG). To explore correlations among variables within each group we performed a multivariate analysis (PCA) on standardized data (centered/scaled) and non-metric dimensional scaling (NMDS) to reduce dimensionality while maximizing the variance (see Table S5 for detailed variables):

- **CLTP (PCA)**: climatic parameters (temperature and water regimes) and topographical variables (aspect and topographical configuration);
- **LT (PCA)**: geochemical composition of major elements after log-ratio transformation to correct for statistical dependency (Van Den Boogaart and Tolosana-Delgado, 2008);
- **SOIL (PCA)**: soil physical (grain size distribution) and chemical properties (pH, delta pH) to capture the main sources of variability in soil characteristics, soil weathering (TRB);
- **VG (NMDS)**: the abundance of each vascular plant species (pinpoint abundance);
- **SOC (PCA)**: SOC chemistry and stability indices (DRIFT and Rock-Eval®). This PCA allowed to obtain a single, standardized SOC biogeochemical stability estimator that maximized the inter-sample variance. We used coordinates on axis 1 of this PCA to assess relative biogeochemical stability. Hereafter, we call this variable **C.stab** (Fig. 4.E).

3.6. Structural equation modelling (SEM)

To quantify direct and indirect causal relationships between climate, topography, parent material, soil properties, vegetation, and their synergistic effects on SOC properties (i.e., stock and stability; Fig. 1.B), we applied structural equation modelling (SEM). We selected variables that best represent the heterogeneity of conditions across the study area and that carry clear ecological meaning. To determine the number of variables to retain from each group, we used Horn's parallel analysis (via the PARAN package, Dinno, 2024), which identifies the number of statistically significant axes in a Principal Component Analysis (PCA). Since variables within a group often exhibit high collinearity, this test helped us determine how many dimensions truly capture the variability of each group. For interpretability, we used actual variables—rather than PCA axis scores—as inputs for the SEM:

- **CLTP:** GDD (axis 1) and DAH (axis 2);
- **LT:** Ca/Si ratio (hereafter called LT_index);
- **SOIL:** TRB, clay/sand ratio (hereafter called Grain) and pH.

For plant composition analysis, we used NMDS from Bray-Curtis distance matrix to capture plot proximity of plant taxonomic composition into two dimensions (axis 1 & 2 of NMDS: **VG_1** & **VG_2**).

As the processes controlling SOC properties are highly dependent of soil depth and the land cover, we split the soil layer in two different groups (0–30 cm and 30–50 cm), and the habitat into non-forested habitats (high elevation grasslands and heathlands) and forested habitats. Thus, we constructed separate SEM models for soil layers and habitat types. Model structure was built according to the scientific literature and are illustrated in Fig. 1.B. Relationships in the models were fitted using the "lme4" package (Bates et al., 2015) and were assumed to be linear. Log- or square-root transformations were applied as needed to meet the assumptions of residual normality and homoscedasticity.

Once model structure was defined and the variables selected, we hypothesized causal relationships represented by directed acyclic graphs. These relationships were then evaluated for consistency with the observed patterns of variance and covariance in the data using piecewise SEM R package (Lefcheck et al., 2023). Climate, topography and parent material were treated as exogenous variables (Fig. 1.B), assuming that these variables cannot be influenced by the other variables of our study. On another hand, SOC properties (i.e., stock and stability), was set as final response variables (Fig. 1.B) that do not influence other variables as our main research aim lies in the responses of SOC properties. Finally, plant and soil properties were intermediate variables within our SEM (Fig. 1.B). We used a d-separation test to check for significant links that were not included in the conceptual model structure (Shipley, 2000). The models were evaluated using the Chi-squared goodness-of-fit test, Fischer test and RMSEA. Standardized effect sizes were estimated by bootstrapping (999 iterations) which allow to determine the significance of each effect and classify them as direct, indirect (partial correlations), or mediators using the "semEff" package (Murphy, 2022). Direct effects

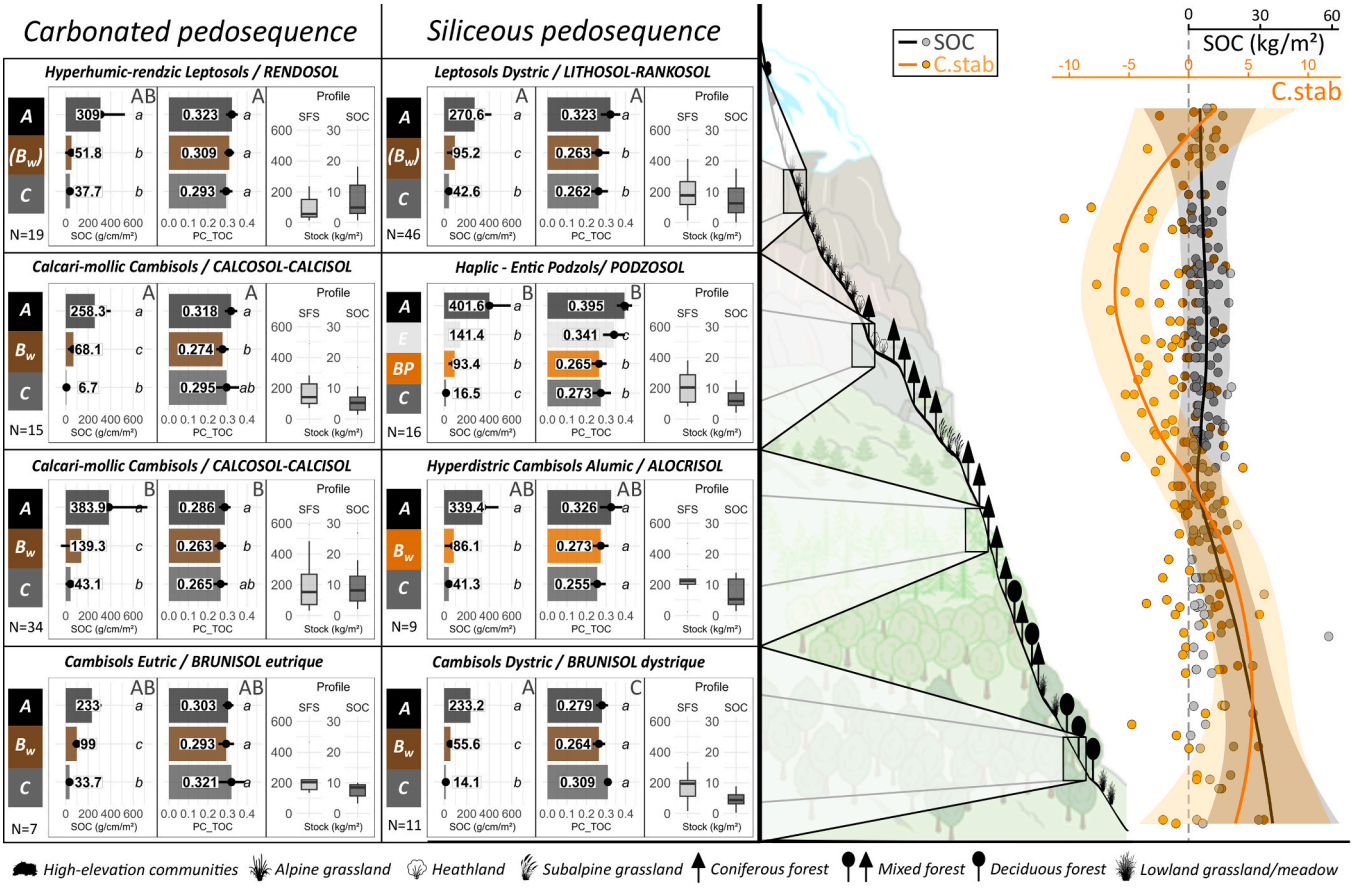

Fig. 3. SOC properties along pedosequences. This figure presents soil organic carbon (SOC) properties at different locations along pedosequences. For each position, the SOC stocks are shown by horizon, with values normalized by horizon thickness to account for variations in thickness. Additionally, an index of SOC biogeochemical stability (PC_TOC) is provided for each horizon. The total fine soil stock (SFS) and overall SOC stocks (SOC) for the entire soil profile are also displayed. This comprehensive view allows for the comparison of SOC distribution, stability, and soil stock dynamics across the pedosequences. Letters indicate significant p-value after post-hoc Tukey HSD test, within profile (lowercase letters) and within pedosequence (capital letters). Orange and black curves represent the loess regression of C.stab index and SOC stocks respectively for the entire profile along the elevation gradient.

were as the sum of the coefficients of each direct path, while indirect effects corresponded to the sum of the coefficients of each indirect path, where the effect for each indirect path is computed as the product of the standardized path coefficients along the path.

4. Results

4.1. Mountain SOC stocks

The correction applied for the fine soil fraction significantly impacted SOC stock estimates, conventional methods tend to overestimate stocks, particularly in soils with a high coarse elements content (Fig. S1.B). Across the entire soil profile, SOC stocks ranged from 0 to 40 kgC/m^2, with most values between 2 and 20 kgC/m^2 (Fig. 3, Table S4). The distribution of SOC within the profile varied by depth (Table 1). In the surface horizon (0–10 cm), SOC stocks were primarily influenced by SOC content (41 %), followed by bulk density (24 %) and coarse element content (5 %). At greater depths (30–50 cm), SOC content remained the dominant factor (42 %), but the influence of bulk density decreased (17 %), while the contribution of coarse elements increased significantly (17 %). An elevation pattern of SOC stocks emerged with an increase with elevation up to the montane belt, relative stability until the subalpine/alpine boundary, and then a decline at higher elevations. SOC stability also declined drastically at the subalpine/alpine transition (Fig. 3).

4.2. Indicators of SOC stability

The analysis of SOC properties across soil horizons revealed significant correlations between different assessment methods. The Aliphatic index (from DRIFT) was positively correlated with the HI index (Rock-Eval®) ($r = 0.35$, $p < 0.001$). Likewise, PC_TOC correlated positively with the Aliphatic index ($r = 0.39$) but negatively correlated with the Carbonyl index ($r = -0.23$) and the Aromatic index ($r = -0.43$). All biogeochemical stability indicators were linked to SOC content: HI, PC_TOC, and the Aliphatic index showed positive correlations, while OI, Txx_yy_zz, and the Aromatic index exhibited negative correlations (Fig. 4.E, Fig. S2). Absolute values for Rock-Eval® indices ranged from 30 to 485 for HI, and from 145 to 638 for OI. DRIFT parameters ranged between 0.19 and 0.52 for the Aliphatic index (relative aliphatic peak area), between 0.30 and 0.49 for the Carbonyl index, and between 0.17 and 0.37 for the Aromatic index. Thus, a wide range of heterogeneous properties were captured with this sample set.

The PCA integrating SOC characterization indicators revealed a stability gradient along axis 1 (Fig. 4.E). This axis was negatively correlated with HI, Aliphatic, and PC_TOC, and positively correlated to Aromatic, Carbonyl, Txx_yy_zz and OI. Axis 1 was thus used as a proxy for SOC biogeochemical stability, with higher values indicating higher stability, as shown by the **C.stab** index in Fig. 4.E. This index was further applied to assess relative SOC stability in subsequent analysis. This index exhibited a clear elevation pattern, significantly declining at the alpine-subalpine transition, though results at extreme elevations were not interpreted due to the limited number of plots at these elevations (Fig. 3, Fig. S4).

Table 1
Variance partitioning for SOC stocks based on three key parameters: SOC concentration, bulk density (BD) and coarse content. Residuals represents the variance not explained by these parameters. Columns correspond to a specific soil horizon: 0–10 cm, 0–30 cm, 30–50 cm, and to the whole soil profile. For the method used to calculate SOC stocks, refer to Fig. S1.

	0–10	0–30	30–50	Profile
—	—	—	—	—
$SOC_{content}$	0.41	0.37	0.42	0.26
—	—	—	—	—
BD	0.24	0.26	0.17	0.33
—	—	—	—	—
Coarse $fragment_{content}$	0.05	0.04	0.17	0.00
—	—	—	—	—
Residuals	0.47	0.49	0.40	0.52
—	—	—	—	—

4.3. Variations of SOC properties along pedosequences

Of the 170 plots, 158 were successfully assigned to a pedosequence (Fig. 1.A; see Table S2 for details). The remaining 12 profiles could not be classified due to distinct pedogenetic processes, such as Gleyic processes (Table S2). Soil horizon properties (Table S4) confirmed the homogeneity of the profiles and the robustness of the classification.

Within each pedosequence, fine soil stock decreased with elevation, though this was not consistently accompanied by a significant reduction in SOC stock, i.e., there was an increase in SOC content (Fig. 3). In the carbonated pedosequence (in Calcari-mollic Cambisols under forest), SOC stock peaked at the subalpine belt, while in the siliceous pedosequence, the peak appeared higher in elevation at the podzolization stage, between the subalpine and alpine belts (Hyperdistric Cambisols Alumic and Podzols). Overall, SOC stocks were comparable between the carbonated and siliceous pedosequences; however, in the upper half of the elevation gradient, they tended to be higher in the carbonated pedosequence (Fig. 3, Table S4). As expected, A horizons contained the largest and most biogeochemically labile SOC stocks. However, SOC biogeochemical stability in A horizons declined with elevation, reaching a minimum at the podzolization stage (2000 – 2500 m a.s.l.) and slightly increased above. Conversely, while deeper horizons contained smaller SOC stocks, their stability was notably higher. Overall, SOC stability was lower in the siliceous pedosequence than in the carbonated pedosequence.

SOC properties were closely linked to pedogenetic processes, as supported by the geochemical horizon weathering analysis. The TRB weathering index correlated with both SOC content and stability (Fig. S3.B). More weathered horizons of our dataset contained higher carbon content ($p < 0.01$). SOC biogeochemical stability initially decreased at early weathering stages but increased beyond a certain threshold.

4.4. Drivers of SOC properties

To identify key SOC drivers, we selected variables that correlated the best with Horn's test significant PCA axes (Fig. 4). For climate and topography (Fig. 4.A), the first axis represented a temperature gradient, with high growing degree days (GDD) and a long growing season at one pole and extended winters at the other. The second axis captured hydric and topographic influences, capturing the perceived solar energy, especially with high DAH values representing high solar exposition to due optimal aspect/slope combination. The positive pole corresponded to northern exposures with high moisture balances (precipitations minus evapotranspiration, water deficit, DEF), indicating higher site humidity, while the negative pole is defined by southern exposures with more heat and high evapotranspiration. We used **GDD** and **DAH** to characterized climate and topography in SEM.

Analysis of the parent materials reveal that the first axis explained 53.7 % of the variance, representing a gradient between calcium-rich rocks and aluminosilicates (Fig. 4.B). The second axis distinguished between ferromagnesian minerals and potassic minerals (e.g., orthoclase). We used Ca/Si ratio (**LT_index**) to characterized lithology in SEM.

Vegetation NMDS was used to display plant taxonomic proximity of plots within a two-dimensional space (Fig. 4.C). Axis 1 (**VG_1**) reflects the elevation gradient, while axis 2 (**VG_2**) represents variations in vegetation driven by substrate type (siliceous −> carbonated).

In PCA of soil properties (Fig. 4.D), the axis 1 explained 52.3 % of the variance and distinguished between an acidic, sandy, and nutrient-poor

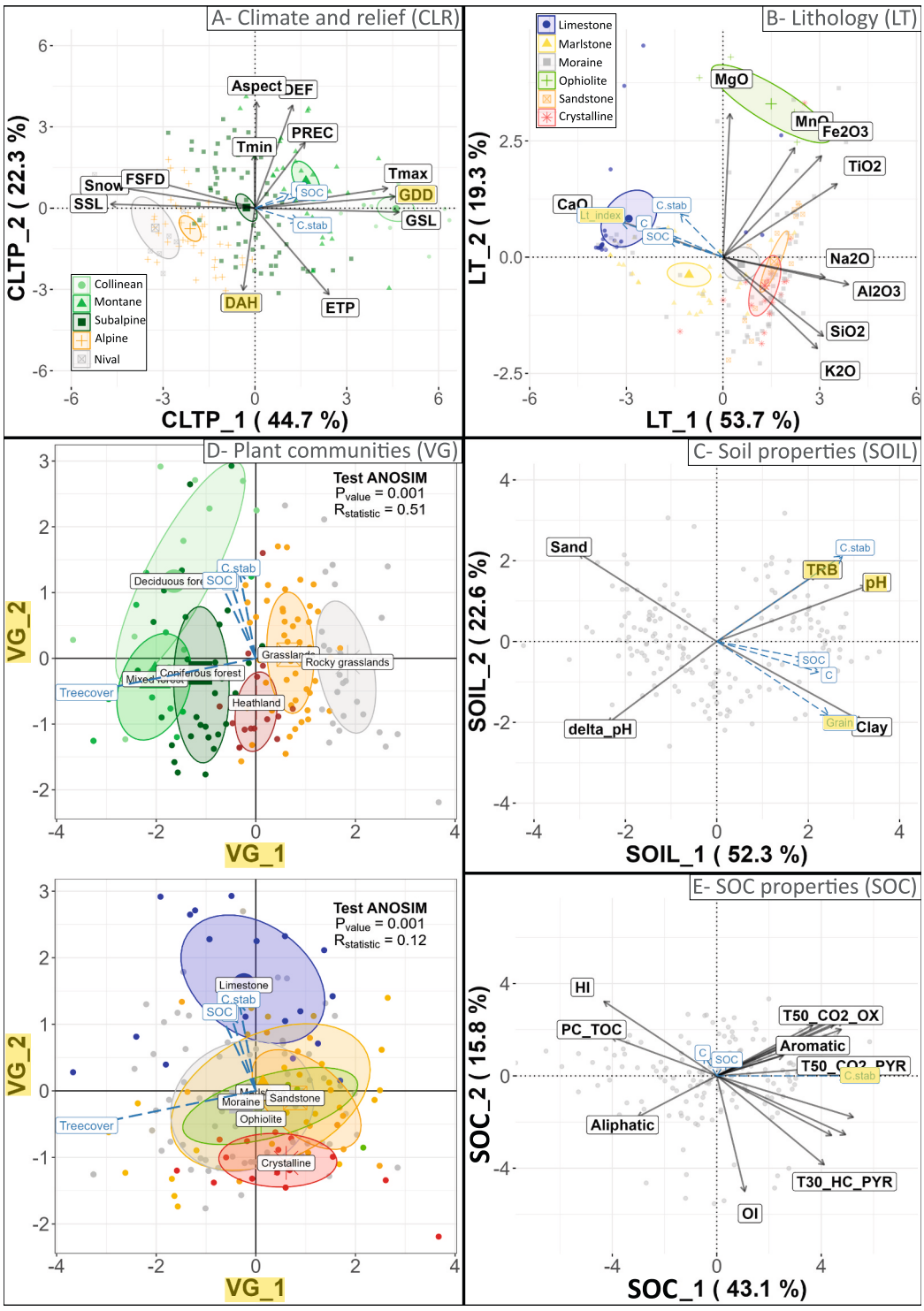

Fig. 4. Variation in CLORPT variables (CLTP, LT, VG, SOIL) represented through PCA or NMDS. Variables selected for structural equation modelling are highlighted in yellow. Blue arrows represent illustrative variables, which were not included in the PCA computation but are projected onto the ordination space for interpretation. See Table S5 for abbreviations correspondence. (A) Climate & topography (CLTP): The first axis (CLTP_1) represents a thermal regime gradient driven by GDD and GSL. The second axis (CLTP_2) captures a hydric gradient, reflecting a north/south opposition (aspect and DAH) and hydric deficit (precipitation minus actual evapotranspiration). For the SEM, we selected **GDD** (growing degree day) for axis 1 and **DAH** (diurnal anisotropic heating) for axis 2. (B) Bedrock geochemistry: Axis 1 of the PCA highlights a gradient between calcium-rich and aluminosilicate-rich bedrock. We used **Lt_index** (CaO/SiO_2) for SEM. (C) Soil properties (0–30 horizon): Axis 1 reveals a gradient of soil alteration, grain size distribution, and fertility (SOIL_1). We used **Grain** index (Clay/Sand ratio), **TRB** (alteration index) and soil **pH** for SEM. (D) NMDS of vegetation composition: Axis 1 (**VG_1**) represents a land cover gradient, while Axis 2 (**VG_2**) captures substrate preference. (E) SOC properties (0–30 horizon): The PCA of SOC properties shows correlations between different indices and methods: DRIFT (Aliphatic and Aromatic index) and Rock-Eval® (Hydrogen index=HI; Oxygen index=OI; proportion of pyrolysable carbon=PC_TOC; thermal indices Txx_yy_zz representing the temperature at which xx% of carbon is released in yy form (HC, CO or CO2) during the zz phase (pyrolysis or oxidation). Axis 1 is used to derive an index of SOC stability (**C.stab**), providing a relative indication of SOC stability between sites.

pole, and a basic, clayey, and nutrient-rich pole. Axis 2 reflected geochemical weathering highlighted by positive relationship with soil weathering index (TRB). We used clay/sand ratio (**Grain**), **pH** water and **TRB** to characterized soil properties in SEM analysis.

SEM analysis confirmed the theoretical framework, with a good global fit (Chi-squared and Fisher test p-values > 0.05 and RMSEA values < 0.06), demonstrating robust alignment with the data (Fig. 5, Fig. S7).

The influence of GDD varied by habitat: in forests, higher GDD increased both SOC stocks and lability, whereas in grasslands, higher GDD correlated with lower SOC stocks and reduced lability (Fig. 5). Diurnal anisotropic heating (DAH) also exerted a strong effect: in non-forested habitats, higher DAH increased SOC stocks (particularly stable SOC), while in forests, it had the opposite effect (Fig. 5).

SEM results confirmed that carbonated rocks (high LT_index) led to higher SOC stocks and greater SOC lability, regardless of habitat type (Fig. 5, S7). In forested habitats, soil properties and lithology had a stronger influence on SOC than in non-forested habitats (Table S3). Greater soil weathering was associated with higher SOC stocks and stability (Fig. 5, S3 and S7). Soil pH negatively correlated with SOC stocks but positively with SOC stability, particularly in surface horizons of non-forested habitats. In forests, soil pH had the opposite effect on SOC stocks (Fig. 5). Grain size has minimal impact in non-forested habitats. However, in forests, clay-rich soils tend to have higher SOC content and greater SOC stability (Fig. 5).

While the elevational-driven vegetation gradient (VG_1) had little impact on SOC, substrate-driven vegetation differences (VG_2) were significant: calciphilic non-forested habitats had higher and more labile SOC, whereas acidic forests had lower SOC stocks with greater lability (Fig. 5 and S7).

5. Discussion

Our study, based on 170 plots, provides a detailed characterization of SOC properties in mountain environments. It highlights the critical need to account for soil coarse elements content to improve SOC stock estimations accurately and explores the SOC biogeochemical stability in these ecosystems. Elevation patterns were evident, with higher SOC stocks observed at the montane level and the subalpine/alpine boundary, alongside a notable decrease in SOC stability at the subalpine/alpine boundary. The findings confirm that CLORPT factors —climate, organisms, relief, parent material, and time (or more precisely, the degree of weathering)— explain a significant portion of SOC variability in both forested and non-forested habitats. These insights lay the groundwork for identifying SOC stocks most vulnerable to the impacts of global warming.

5.1. Signature of mountain SOC stocks

Our results indicate SOC stocks ranging from 0 to 10 kgC/m^2,

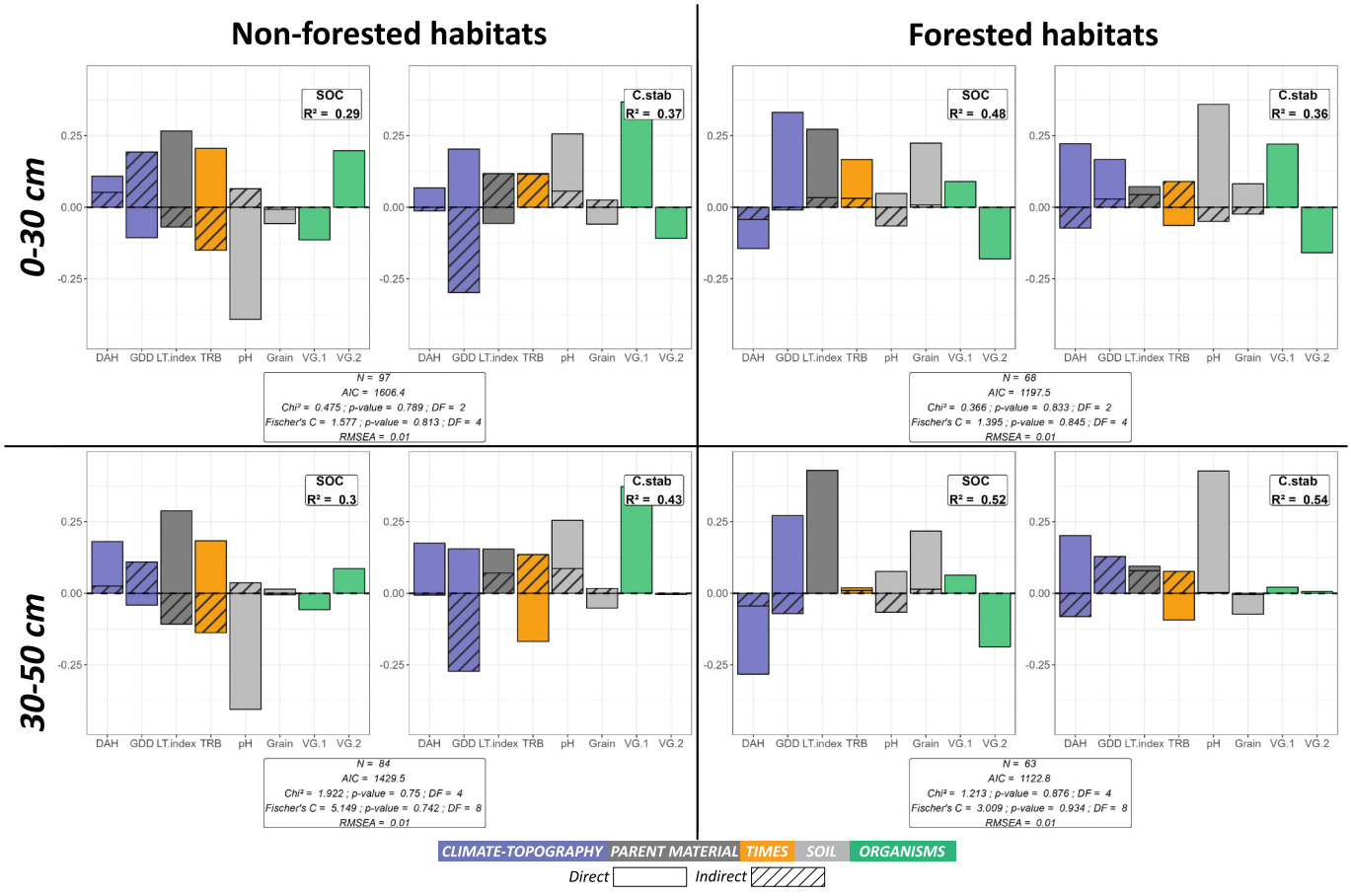

Fig. 5. Standardized estimates of predictors of SOC stocks (SOC) and SOC stability (C.stab). SEMs were used to analyze the controls on SOC properties, distinguishing between non-forested habitats and forested habitats, as well as the 0–30 cm and 30–50 cm soil horizons. The models follow the conceptual framework introduced in Fig. 1, with their structure compared to our data. Model fit was evaluated using global SEM adjustment metrics, including the Chi-squared test, Fisher's test, and RMSEA. A D-separation test was performed to assess whether any significant relationships were omitted. The figure presents the proportion of absolute direct and indirect effects on SOC stocks and SOC stability. Variables related to CLTP represent climate-driven stabilization, LT and SOIL refer to organo-mineral interactions, and VG captures chemical recalcitrance. "Time" reflects the soil's weathering state. For a detailed breakdown of direct, indirect, and mediated effects on SOC content and stability, refer to Fig. S7.

reaching 20–40 kgC/m^2 in the most extreme cases (Fig. 3). These findings align with previous studies; for example, stock estimates for France suggest a range of 7.5 to 17.5 kgC/m^2 (Mulder et al., 2016). In the same study, SOC stocks in surrounding lowland soils were estimated between 1 and 5 kgC/m^2. However, in this study, as in other large scale soil monitoring (RMQS, 2017), mountain soils were heavily under-sampled. Our study therefore filled this gap. Overestimation in model predictions may also stem from inadequate integration of coarse elements content, which is particularly high in mountainous ecosystems. Our correction methods, while including some biases (e.g., from visual estimation), yielded more realistic SOC estimates (Fig. S1), effectively halving the measured stocks (Poeplau et al., 2017). However, estimating coarse elements content remains particularly challenging and is often overlooked. Future research should aim to incorporate this parameter for improved SOC stock estimation, especially in mountain soils where coarse elements content is particularly high (Leifeld et al., 2005).

Up to a certain threshold in elevation, previous studies reported an increase in SOC stocks with elevation (Meng et al., 2019), estimated at around 0.31 kgC/m^2 per 100 m for grassland soils and 0.45 kgC/m^2 per 100 m for forest soils (Sjögersten et al., 2011). This trend was largely attributed to the progressive reduction in organic matter decomposition rates and the accumulation of partially decomposed organic residues, driven in temperate mountains by increased precipitation and lower temperatures with increasing elevation (Zhang et al., 2025). However, beyond a certain elevation plateau —where biomass production becomes limited by climatic conditions— this relationship no longer holds (Bardgett, 2005; Bojko and Kabala, 2017; Meng et al., 2019). In Europe, this threshold is between 1 500 – 2 000 m, corresponding to the forest-grassland ecotone (Bardgett, 2005; Bojko and Kabala, 2017; Djukic et al., 2010). This interpretation is consistent with our results (Fig. 3).

5.2. Signature of mountain SOC stability

The complex controls on mountain SOC are observed beyond stocks, with composition and stability. Interestingly, both methods of SOC characterization (DRIFT and Rock-Eval®) show a good correlation in their indices (Fig. 4.E, Fig. S2). We observed that the samples exhibit either both hydrogen-rich composition with aliphatic bonds and low thermal stability or both oxygen-rich composition and high thermal stability. This observation suggests three possible hypotheses. One hypothesis proposes that the Rock-Eval® analysis method is highly influenced by the chemical composition of SOC. In this case, thermal indicators may primarily reflect chemical characteristics rather than capturing other SOC stabilization factors, such as organo-mineral interactions. This explanation is unlikely according to Cécillon et al. (2018) and Saenger et al. (2015) who conducted a thorough comparison of SOC partitioning methods.

A second hypothesis is that chemical recalcitrance serves as an important stabilizing factor in mountain ecosystems (Zhongsheng et al., 2023). Although the significance of this parameter is widely debated (Schmidt et al., 2011), the climatic conditions in these environments may amplify its role. While the mean residence time of SOC does not vary significantly with molecular composition in warmer ecosystems (Amelung et al., 2008), it is possible that in cold ecosystems, limited temperature prevents microorganisms from degrading certain molecular types, resulting in stabilization due to both chemical properties and climate conditions. Furthermore, as the overall mean residence time of SOC is substantially extended in cold environments, a small difference in residence time between molecule groups in warmer ecosystems could become considerably more pronounced in these settings. This climatic stabilization is reminiscent of what it is observed in allophane soil where organic matter complex with SRO minerals, and could be long-term stabilized while it presents low thermal stability (Stoner et al., 2023).

Thirdly, the relative proportion of aliphatic compounds tends to decrease with the microbial transformation of organic matter (Davidson & Janssens, 2006). Microbially transformed organic matter is also more likely to associate with mineral surfaces, particularly when compared to fresh plant litter, which retains a stronger aliphatic signature. As a result, soils with higher proportions of mineral-associated organic matter (MAOM) typically exhibit a weaker aliphatic signal and, conversely, higher thermal stability.

Our results contrasted with those of Delahaie et al., (2023), who reported higher hydrogen index (HI) values—a proxy for SOM lability—for forests than for grasslands (240 and 229, respectively), whereas in our study, HI values were lower for forests (201) and higher for grasslands (258), suggesting lower biogeochemical stability in mountain grasslands compared to lowland ecosystems. Similarly, in terms of thermal stability indices, Delahaie et al., (2023) observed T50_CO2_OX values of 410 °C and 409 °C for forests and grasslands respectively, whereas our findings indicate values of 404 °C and 399 °C. (Table S2).

Several studies have reported an accumulation of labile and particulate organic residues in high-elevation soils (Bonfanti et al., 2025d; Budge et al., 2011; Leifeld et al., 2009). Correlations between elevation and SOC lability indicators suggest the existence of a biogeochemical stability gradient (Sjögersten et al., 2011). A simultaneous increase in O-alkyl C content and decrease in alkyl C content with elevation imply a reduction in decomposition rates at higher elevations (Djukic et al., 2010; Xu et al., 2014). Additionally, Budge et al. (2011) showed that particulate organic matter (unbound to mineral phases) accounted for 40–58 % of total organic carbon (TOC) in grassland soils between 2 200 m and 2 700 m, compared to only 7–30 % in soils between 400 m and 1 900 m reported by Leifeld et al. (2009). Additionally, SOC stabilization in the Pyrenean mountains, as measured by laboratory incubation, was lower at the coldest sites (Garcia-Pausas et al., 2007). Pedogenesis and SOC properties.

Many studies challenged the elevation-SOC stock relationship (Bangroo et al., 2017; Britton et al., 2011; Leifeld et al., 2009). They proposed that the elevational distribution of SOC stocks and stability likely arises from the interplay between productivity and mineralization rates, both of which vary with elevation (Figs. 6 & S6). While productivity and mineralization rates decrease with elevation, the drivers behind these processes differ: productivity depends primarily on light intensity and temperature (Körner and Paulsen, 2004), whereas mineralization is strongly temperature-dependent. This dynamic results in large labile SOC stocks in the lower alpine and subalpine zones, where relatively long growing seasons combine with low temperatures, slowing decomposition, although there is considerable spatial variability within this zone.

Elevation, however, is not an optimal parameter for studying SOC distribution, as climate-elevation relationship is modulated by exposure, topography, and microtopography that significantly influence growing season length and GDD (Choler, 2005). Pedoclimate offers a more robust framework, accounting for factors that modulate soil climate (Egli et al., 2009; Kemppinen et al., 2024; Patton et al., 2019). In the same way, to analyze SOC properties along elevation gradients effectively, pedosequences are more suitable as they integrate multiple SOC drivers. The concept of the pedological taxon is therefore most meaningful, as it integrates SOC drivers holistically. Given the significant differences in pedogenesis on acidic versus alkaline substrates, we propose two distinct pedosequences, highlighting the strong geological control over SOC properties, as reported by previous studies (Barré et al., 2017, see Lt_index in Fig. S7).

Our results demonstrate that SOC stocks and stability are higher in carbonated pedosequences than in siliceous ones (Fig. 3, Table S4, Fig. S4.D). This finding aligns with previous studies showing that SOC stocks are significantly greater in limestone soils (Doetterl et al., 2015; Leifeld et al., 2009) compared to those formed on acidic igneous rocks (Pan et al., 2024; Yang et al., 2020). The difference is attributed to distinct stabilization mechanisms: while both soil types stabilize SOC through complexation with Fe and Al oxides, limestone soils gain additional stabilization from Ca interactions. Additionally, Liao et al. (2020) showed that carbon fluxes were higher in carbonate-rich

environments than in siliceous ones, driven by increased fertility, productivity, and mineralization rates (Heckman et al., 2009), resulting in higher SOC stocks, especially stable stocks (Fig. S4).

Soil stabilization processes vary by horizon and soil type. In Podzols, stabilization in the BP horizons primarily occurs through complexation with Al and Fe (Krettek et al., 2020; Schulze et al., 2009), whereas in the A and E horizons, pH plays a dominant role (see Soil pH section). In carbonate soils (Calcari-mollic Cambisols), stabilization is largely due to complexation with Ca (Rowley et al., 2018). In Cambisols, stabilization is driven by clay interactions, as demonstrated by Soucémarianadin et al., (2019) and Delahaie et al., (2023), who found strong correlations between clay content and hydrogen index (HI) ($r = -0.35$, $p < 0.01$), and thermal stability indices (e.g., T50_CO2_PYR, $r = 0.56$, $p < 0.01$). Since weathering processes release stabilizing agents such as Ca, Al, Fe, and clay minerals, the degree of soil weathering plays a key role in determining SOC stabilization—specifically, the relative proportions of mineral-associated organic carbon (MAOC) versus particulate organic carbon (POC). In contrast, in poorly developed highland soils such as Leptosols, SOC stabilization is more likely controlled by external environmental conditions, especially climate, due to the limited availability of reactive mineral surfaces.

5.3. Soil weathering

Pedosequences provide a unique framework to assess the processes of soil weathering, which can be effectively analyzed using the weathering index (TRB). An elevation gradient exists in soil development, with younger, less developed soils at higher elevations —mainly due to recent deglaciation— and more mature, altered soils at lower elevations (Brosens et al., 2021; Egli et al., 2006). This is confirmed by the decrease of our weathering index with elevation (TRB, Table S4). However, local factors may modulate this soil weathering gradient, particularly rejuvenation processes, such as gravitational events (e.g., solifluxion, scree) and legacy effects (Delgado-Baquerizo et al., 2017). Our approach assesses the soil weathering state rather than soil age. As such, the functional state of the soil, including its weathering sensitivity, its reservoir of mineral nutrients, and its pool of mineral particles available for SOC interactions are explicitly considered. However, possible legacy effects, such as past land use and climate change, were not considered, though these factors can significantly impact SOC properties (Canedoli et al., 2020; Delgado-Baquerizo et al., 2017; Guidi et al., 2014). It is important to note that while this index is a useful tool, it is not a perfect measure of soil age. Instead, it more accurately reflects the extent of weathering, which depends on both parent material type and climate. Additionally, external factors such as atmospheric or aeolian deposits, periglacial cover beds, and past landslide events could have introduced material from other locations, potentially affecting the validity of the TRB index in our study area. However, our study reasonably assumed that these processes were minimal at the study sites under consideration.

Our results indicate that the most weathered soils of our study area exhibit the highest SOC stocks (Fig. 5, Fig. S3). This finding aligns with studies conducted along chronosequences (Khedim et al., 2021; Laliberté et al., 2013), and with those employing weathering indices, such as TRB (Doetterl et al., 2015). In well-developed soils, a greater availability of minerals enables stronger interactions with organic matter, promoting its stabilization. Additionally, soil development fosters the formation of the soil structure, which can further stabilize SOC within aggregates (John et al., 2005; Virto et al., 2010). Enhanced weathering supports organo-mineral interactions, facilitating carbon stabilization. The most altered soils are found in the oldest ecosystems, which have had more time to accumulate carbon and increase the quantity of particles capable of stabilizing SOC. As a result, their most stable carbon reservoirs, particularly mineral-associated organic carbon (MAOC), are more fully saturated. Additionally, our results demonstrate that clay content has a stronger influence on SOC stocks and stability in lowlands, forested habitats compared to high, non-forested habitats (Fig. 5). This finding reinforces the idea that organo-mineral interactions play a more significant role in SOC stabilization at lower elevations. It is important to note that, within the context of this study, even the most weathered soils may appear relatively young compared to tropical soils, where advanced weathering can have the opposite effect on O-M stabilization due to the depletion of ions and minerals that contribute to stabilization. In such tropical contexts, an inverse relationship between weathering state and SOC stability has been observed (Laliberté et al., 2013).

Finally, according to the theory of ecosystem retrogression, nitrogen is the primary limiting factor for productivity in young soils, whereas in older or more weathered soils, phosphorus becomes increasingly limiting. This is because phosphorus is mainly derived from the weathering of parent material and becomes scarce as weathering progresses and the P reserve in the parent material is depleted (Laliberté et al., 2013; Vitousek and Farrington, 1997). This theory implies a nutrient optimum at mid-elevations (Thébault et al., 2014), where N_2 fixation and apatite weathering occur simultaneously. We suggested that this balance may also explain the higher SOC stocks observed at mid-elevations. This field of research remains relatively unexplored in alpine environments, making it crucial to deepen our understanding of nutrient limitations, particularly to better understand SOC stability (Bueno De Mesquita et al., 2020).

5.4. Soil pH

SOC properties were driven by both lithology and weathering state, as one of their derivative variables, soil pH. This integrative variable regulates parameters involved in the carbon cycle, such as microbial activity, enzymatic function (Puissant et al., 2019), microbial community composition (Martinez-Almoyna et al., 2022), and plant productivity (Liao et al., 2020). Additionally, pH is interdependent with, and thus correlated to, other factors that further modulate the carbon cycle, including soil fertility (base and nutrient content), the abundance of stabilizing elements (e.g., oxyhydroxides, calcium), and floristic composition, which influences the chemical nature of SOC inputs that further modulate soil pH. These relationships are reflected in the alignment between our conceptual model and empirical data (Figs. 5 & S7).

We observed a negative relationship between soil pH and SOC stocks as found by Meng et al. (2019). We also found that soil pH had a positive effect on SOC stability (Fig. 5), which is consistent with Delahaie et al. (2023), who found a negative correlation between soil acidity and thermal stability indices (T50_CO2_PYR; $r = -0.73$, $p < 0.001$), and a positive correlation with hydrogen index (HI; $r = 0.42$, $p < 0.001$). These studies proposed that soil acidity may protect SOC from microbial degradation by limiting microbial activity and reducing SOC mineralization. Additionally, this aligns with the AMG model —a two-compartment model of SOC stability— in which mineralization is highly pH-dependent, with a marked increase between pH 5.5 and 7 (Clivot et al., 2019). These values represent the “window of opportunity” for microbial decomposition proposed by Rowley et al., (2018); below this range, low pH limits microbial activity and favorizes Al/Fe interactions with SOC, and above it, Ca complexation stabilizes SOC. The stabilizing effect of soil pH is thus particularly important in acidic and decarbonated soils.

5.5. SOC stabilization and vulnerability with climate change

Not all studies have reached a consensus on drivers of SOC stocks, and few account for the variability in rock types, vegetation, and climate. One of the key findings of our study is the validation of our conceptual model (Fig. 5, Table S3), illustrating the idea that the persistence of soil organic matter is an intrinsic property of the ecosystem (Schmidt et al., 2011).

Examining a broad range of soils and vegetation types across various

biomes, Jobbagy and Jackson (2000) found that SOC content was positively correlated with annual precipitation and clay content, but negatively correlated with annual mean temperature. Similarly, Amundson (2001), by compiling data from multiple studies, proposed an empirical equation that highlighted a strong correlation between SOC stocks, mean annual air temperature, and mean annual precipitation (R^2 = 0.65). This was further corroborated at a smaller spatial scale by Delahaie et al. (2023), who found that mean annual temperature (MAT) was positively related to thermal stability indices (e.g., T50_CO2_PYR), and negatively related to hydrogen index (HI) in mainland France soils. Climate role was also highlighted by other previous studies who showed a significant climate stabilization in high-elevation grasslands (Bonfanti et al., 2025c; Budge et al., 2011; Djukic et al., 2010).

Our findings align with these observations (e.g., C.stab ~ GDD in Fig. 5). Since MAT does not adequately capture the temperature dynamics in mountainous areas with pronounced seasonality, we used GDD to characterize the temperature regime. The contrasting effects of growing degree days (GDD) on SOC stocks between high-elevation non-forested habitats (GDD: 290–2000 °C, mean 950 ± 300 °C) and low-elevation forested habitats (GDD: 1040–3900 °C, mean 1860 ± 640 °C) support the idea that lower temperatures at higher elevations promote SOC stabilization (Fig. 5). It suggests that at higher elevations, lower GDD limits decomposition activity, resulting in climate-driven SOC stabilization. Conversely, at lower elevations, when GDD is low, it restricts primary productivity more than decomposition, thereby impeding SOC accumulation (Fig. 5).

The elevation distribution of SOC stocks revealed two peaks: one in the montane zone and another at the subalpine-alpine boundary (Fig. 3). SOC biogeochemical stability remained consistent across the collinean, montane, and lower subalpine levels, as well as in the upper alpine and nival belts. However, a marked decrease in thermal stability was observed between the upper subalpine and lower alpine levels (Figs. 3 and 6). This suggests that, at lower elevations, more developed soils may promote SOC-stabilizing organo-mineral interactions, while soils at higher elevations are less developed, but colder temperatures constrain mineralization, limiting SOC breakdown.

Based on the observations above, ecosystems in the lower alpine zone appear to be the most vulnerable to short-term global warming (see §§ Signature of mountain SOC stocks, Signature of mountain SOC stability, Soil weathering), and in particular, alpine grasslands with soil pH values between 5 and 7 (see § Soil pH). In these ecosystems, SOC stabilization is largely climate-dependent due to poorly developed soils

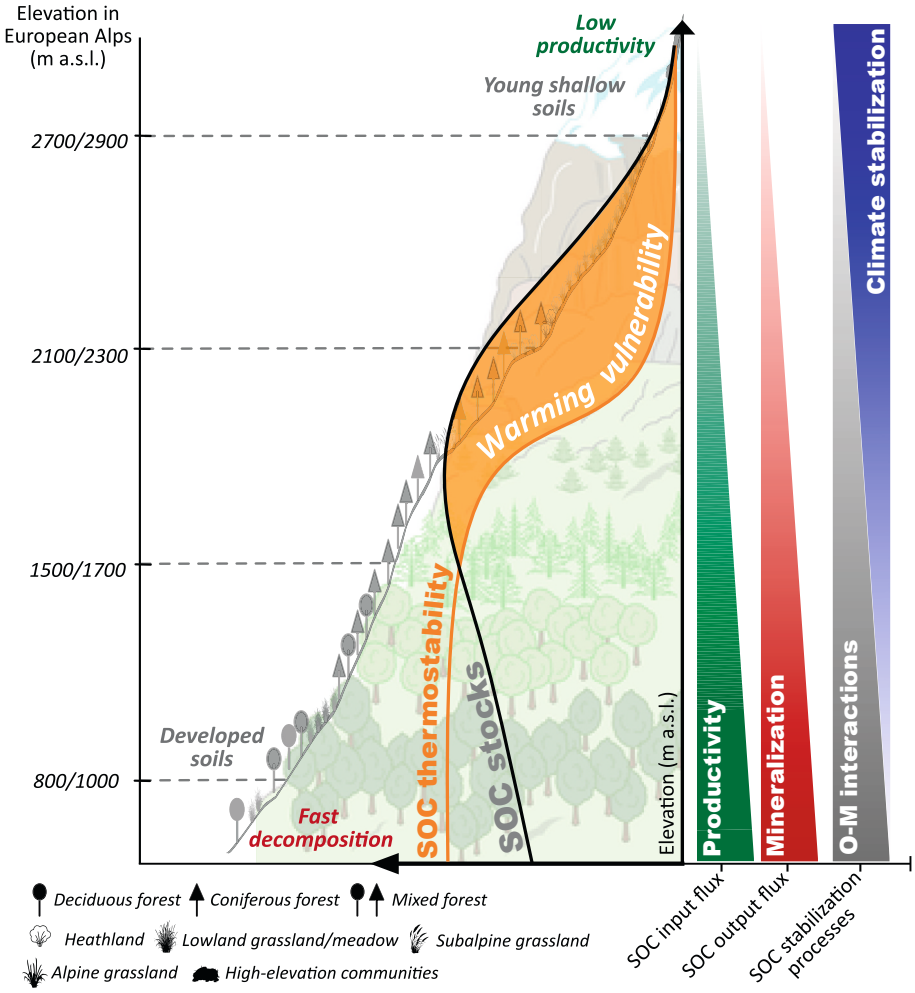

Fig. 6. This study reveals elevation-driven patterns in SOC properties. SOC stocks are highest at the montane level and at the subalpine/alpine boundary, with a marked decrease in SOC stability at the subalpine/alpine boundary. At high elevations, climate predominantly drives SOC dynamics, whereas lithology and soil weathering gain importance at lower elevations. Harsh climatic conditions at higher elevations foster SOC stabilization through reduced decomposition activity, while less developed soils limit organo-mineral interactions. Conversely, at lower elevations with warmer climates, more developed soils facilitate organo-mineral interactions, enhancing long-term SOC storage. Moreover, reduced GDD at high elevations limit both decomposition and productivity, leading to low SOC inputs and climate-driven stabilization (Fig. S6). At lower elevations, higher GDD accelerates SOC fluxes, particularly mineralization. Intermediate elevations, where GDD is insufficient to drive mineralization to the same extent as productivity, promote labile carbon accumulation. Alpine grasslands, characterized by substantial labile SOC stocks stabilized by low temperatures, appear especially vulnerable to climate warming.

with limited organo-mineral associations. At the same time, SOC inputs remain significant, and soil pH conditions may promote optimal microbial activity—especially if rising temperatures further enhance microbial processes (Fig. 6).

6. Conclusion

Our study analyzed the factors influencing SOC properties in mountain environments, highlighting the importance of accurately integrating soil coarse elements content, which is critical for accurate SOC stock estimations in mountainous regions. Accurately integrating this parameter is essential for reliable SOC stock quantification and should be systematically considered in SOC mapping efforts for mountainous regions. The study confirmed that the CLORPT factors (Climate, Organisms, Relief, Parent Material, and Time) account for a significant portion of SOC variability in both non-forested habitats and forests. Using data from 170 plots distributed across 29 elevation gradients, we observed that SOC stocks increased with elevation up to the montane belt, remained relatively stable until the subalpine/alpine boundary, and then declined at higher elevations. SOC stability also declined drastically at the subalpine/alpine transition. In high-elevation areas, climate plays a dominant role, whereas lithology and the degree of weathering become more influential at lower elevations. These findings imply that, at higher elevations, harsh climatic conditions contribute to SOC climatic stabilization, while less developed soils limit organo-mineral interactions. Conversely, in warmer, lower-elevation ecosystems with higher carbon fluxes, more developed soils support greater organo-mineral interactions, which can enhance long-term SOC storage. Alpine grasslands, where climatic stabilization is predominant, appear to be particularly vulnerable to climate warming as they contain large stocks of labile SOC stabilized primarily by low temperatures. As such, they warrant focused attention to better understand their potential response and trajectory under ongoing global warming.

CRediT authorship contribution statement

Nicolas Bonfanti: Formal analysis, Visualization, Writing – original draft, Writing – review & editing, Data curation, Methodology, Software, Investigation. **Philippe Choler:** Conceptualization, Supervision, Validation, Writing – review & editing, Methodology, Resources. **Norine Khedim:** Data curation, Investigation, Software, Formal analysis. **Jean-Christophe Clément:** Writing – review & editing, Supervision, Validation. **Pierre Barré:** Writing – review & editing, Methodology, Supervision, Validation. **Romain Goury:** Writing – review & editing, Software. **François Baudin:** Resources, Writing – review & editing, Methodology, Validation. **Lauric Cécillon:** Investigation, Conceptualization, Methodology, Resources, Supervision. **Amélie Saillard:** Resources, Project administration, Data curation, Conceptualization, Methodology. **Thuiller Wilfried:** Resources, Project administration, Writing – review & editing, Funding acquisition, Methodology, Investigation, Validation, Conceptualization. **Poulenard Jerome:** Writing – review & editing, Investigation, Methodology, Validation, Funding acquisition, Supervision, Resources, Conceptualization, Project administration.

Declaration of competing interest

The authors declare the following financial interests/personal relationships which may be considered as potential competing interests: Nicolas BONFANTI reports financial support was provided by French National Research Agency. Nicolas BONFANTI reports financial support was provided by Department of Isere. Nicolas BONFANTI reports financial support was provided by French Biodiversity Office. Nicolas BONFANTI reports financial support was provided by Grenoble Alpes Metropole. If there are other authors, they declare that they have no known competing financial interests or personal relationships that could have appeared to influence the work reported in this paper.

Acknowledgments

This study was funded by the French Biodiversity Office, France through Sentinelle des Alpes, the Isere department and Grenoble Metro. We also thank all the partners of the Orchamp consortium that contribute to data collection and site maintenance. This work was also supported by the French National Research Agency (ANR), France through the TransAlp project (ANR-20-CE02-0021), which funded the salaries of some of the co-authors. We acknowledge the LTSER Zone Atelier Alpes (programme Solorchamp). We thank Florence Savignac for their support with the Rock-Eval® thermal analysis of soil samples. We also thank all those who took part in soil sampling: Manon Bajard, Lise Marchal, Erwan Messager, Emmanuel Malet, Maeva Cathala, Stéphane Marpot, Alexandre Hallez and Laure Soucémarianadin.

Appendix A. Supplementary data

Supplementary data to this article can be found online at https://doi.org/10.1016/j.geoderma.2025.117452.

Data availability

The data is available at the following link: https://orchamp.osug.fr/

References

AFES, A. française pour l'étude des sols, 2008. Référentiel pédologique 2008 435.
Amelung, W., Brodowski, S., Sandhage-Hofmann, A., Bol, R., 2008. Chapter 6 combining biomarker with stable isotope analyses for assessing the transformation and turnover of soil organic matter. In: Advances in Agronomy. Academic Press, pp. 155–250. https://doi.org/10.1016/S0065-2113(08)00606-8.
Amundson, R., 2001. The Carbon Budget in Soils. Annu. Rev. Earth Planet. Sci. 29, 535–562. https://doi.org/10.1146/annurev.earth.29.1.535.
Bangroo, S.A., Najar, G.R., Rasool, A., 2017. Effect of altitude and aspect on soil organic carbon and nitrogen stocks in the Himalayan Mawer Forest Range. Catena 158, 63–68. https://doi.org/10.1016/j.catena.2017.06.017.
Bardgett, R., 2005. The Biology of Soil: A Community and Ecosystem Approach. OUP Oxford.
Barré, P., Cecillon, L., Kanari, E., 2023. Chap. 10 - Characterization and evaluation of the stabilit of soil organic matter. In Baudin F. (coord). The Rock-Eval method. Principles and application. ISTE-Wiley, 181-207.
Barré, P., Durand, H., Chenu, C., Meunier, P., Montagne, D., Castel, G., Billiou, D., Soucémarianadin, L., Cécillon, L., 2017. Geological control of soil organic carbon and nitrogen stocks at the landscape scale. Geoderma 285, 50–56. https://doi.org/10.1016/j.geoderma.2016.09.029.
Barré, P., Plante, A., Cécillon, L., Lutfalla, S., Baudin, F., Bernard, S., Christensen, B., Eglin, T., Fernandez, J., HOUOT, S., Kätterer, T., Guillou, C., Macdonald, A., Oort, F., Chenu, C., 2016. The energetic and chemical signatures of persistent soil organic matter. Biogeochemistry 130, 1–12. https://doi.org/10.1007/s10533-016-0246-0.
Bates, D., Mächler, M., Bolker, B., Walker, S., 2015. Fitting Linear Mixed-Effects Models using **lme4**. J. Stat. Softw. 67. https://doi.org/10.18637/jss.v067.i01.
Batjes, N. h., 1996. Total carbon and nitrogen in the soils of the world. Eur. J. Soil Sci. 47, 151–163. https://doi.org/10.1111/j.1365-2389.1996.tb01386.x.
Baudin, F., 2023. The Rock-Eval Method: Principles and Application. John Wiley & Sons., Willey. ed.
Benayas, J.M.R., Sánchez-Colomer, M.G., Escudero, A., 2004. Landscape- and field-scale control of spatial variation of soil properties in Mediterranean montane meadows. Biogeochemistry 69, 207–225. https://doi.org/10.1023/B:BIOG.0000031047.12083.d4.
Bishop, T.F.A., McBratney, A.B., Laslett, G.M., 1999. Modelling soil attribute depth functions with equal-area quadratic smoothing splines. Geoderma 91, 27–45. https://doi.org/10.1016/S0016-7061(99)00003-8.
Bojko, O., Kabala, C., 2017. Organic carbon pools in mountain soils — sources of variability and predicted changes in relation to climate and land use changes. Catena 149, 209–220. https://doi.org/10.1016/j.catena.2016.09.022.
Bonfanti, N., Clement, J.-C., Millery-Vigues, A., Münkemüller, T., Perrette, Y., Poulenard, J., 2025a. Seasonal Mineralisation of Organic Matter in Alpine Soils and responses to Global Warming: an In Vitro Approach. Eur. J. Soil Sci. 76, e70050. https://doi.org/10.1111/ejss.70050.
Bonfanti, N., Clément, J.-C., Münkemüller, T., Barré, P., Baudin, F., Poulenard, J., 2025b. Prolonged warming leads to carbon depletion and increases nutrient availability in alpine soils. Appl. Soil Ecol. 213, 106239. https://doi.org/10.1016/j.apsoil.2025.106239.

Bonfanti, N., Poulenard, J., Barre, P., Baudin, F., Voisin, D., Clement, J.-C., 2025c. Seasonality Alters Soil Organic Matter Properties in Alpine and Subalpine Grasslands. Ecosystems 28, 29. https://doi.org/10.1007/s10021-025-00971-y.
Bonfanti, N., Poulenard, J., Clément, J.-C., Barré, P., Baudin, F., Turtureanu, P.D., Pușcaș, M., Saillard, A., Raguet, P., Hurdu, B.-I., Choler, P., 2025d. Influence of snow cover and microclimate on soil organic carbon stability in European mountain grasslands. Catena 250, 108744. https://doi.org/10.1016/j.catena.2025.108744.
BRGM, 2005. Cartes géologiques départementales à 1/50 000 (Bd Charm-50) | InfoTerre [WWW Document]. InfoTerre - BRGM. URL http://infoterre.brgm.fr/formulaire/telechargement-cartes-geologiques-departementales-150-000-bd-charm-50 (accessed 3.10.21).
Britton, A.J., Helliwell, R.C., Lilly, A., Dawson, L., Fisher, J.M., Coull, M., Ross, J., 2011. An integrated assessment of ecosystem carbon pools and fluxes across an oceanic alpine toposequence. Plant and Soil 345, 287–302. https://doi.org/10.1007/s11104-011-0781-3.
Brosens, L., Robinet, J., Pelckmans, I., Ameijeiras-Mariño, Y., Govers, G., Opfergelt, S., Minella, J.P.G., Vanderborght, J., 2021. Have land use and land cover change affected soil thickness and weathering degree in a subtropical region in Southern Brazil? Insights from applied mid-infrared spectroscopy. Catena 207, 105698. https://doi.org/10.1016/j.catena.2021.105698.
Budge, K., Leifeld, J., Hiltbrunner, E., Fuhrer, J., 2011. Alpine grassland soils contain large proportion of labile carbon but indicate long turnover times. Biogeosciences 8, 1911–1923. https://doi.org/10.5194/bg-8-1911-2011.
Bueno De Mesquita, C.P., Brigham, L.M., Sommers, P., Porazinska, D.L., Farrer, E.C., Darcy, J.L., Suding, K.N., Schmidt, S.K., 2020. Evidence for phosphorus limitation in high-elevation unvegetated soils, Niwot Ridge, Colorado. Biogeochemistry 147, 1–13. https://doi.org/10.1007/s10533-019-00624-y.
Burke, I.C., Lauenroth, W.K., Riggle, R., Brannen, P., Madigan, B., Beard, S., 1999. Spatial Variability of Soil Properties in the Shortgrass Steppe: the Relative Importance of Topography, Grazing, Microsite, and Plant Species in Controlling Spatial patterns. Ecosystems 2, 422–438. https://doi.org/10.1007/s100219900091.
Canedoli, C., Ferrè, C., Abu El Khair, D., Comolli, R., Liga, C., Mazzucchelli, F., Proietto, A., Rota, N., Colombo, G., Bassano, B., Viterbi, R., Padoa-Schioppa, E., 2020. Evaluation of ecosystem services in a protected mountain area: Soil organic carbon stock and biodiversity in alpine forests and grasslands. Ecosyst. Serv. 44, 101135. https://doi.org/10.1016/j.ecoser.2020.101135.
Cécillon, L., Baudin, F., Chenu, C., Houot, S., Jolivet, R., Kätterer, T., Lutfalla, S., Macdonald, A., van Oort, F., Plante, A.F., Savignac, F., Soucémarianadin, L.N., Barré, P., 2018. A model based on Rock-Eval thermal analysis to quantify the size of the centennially persistent organic carbon pool in temperate soils. Biogeosciences 15, 2835–2849. https://doi.org/10.5194/bg-15-2835-2018.
Choler, P., 2023. Above-treeline ecosystems facing drought: lessons from the 2022 European summer heat wave. Biogeosciences 20, 4259–4272. https://doi.org/10.5194/bg-20-4259-2023.
Choler, P., 2005. Consistent Shifts in Alpine Plant Traits along a Mesotopographical Gradient. Arct. Antarct. Alp. Res. 37, 444–453. https://doi.org/10.1657/1523-0430(2005)037[0444:CSIAPT]2.0.CO;2.
Clivot, H., Mouny, J.-C., Duparque, A., Dinh, J.-L., Denoroy, P., Houot, S., Vertès, F., Trochard, R., Bouthier, A., Sagot, S., Mary, B., 2019. Modeling soil organic carbon evolution in long-term arable experiments with AMG model. Environ Model Softw. 118, 99–113. https://doi.org/10.1016/j.envsoft.2019.04.004.
Copernicus, 2020. Tree Cover Density 2018 (raster 100 m), Europe, 3-yearly, Sep. 2020 [WWW Document]. EEA Geospatial Data Cat. URL https://sdi.eea.europa.eu/catalogue/copernicus/api/records/c7bf34ea-755c-4dbd-85b6-4efc5fd302a2 (accessed 12.20.23).
Copernicus, 2018. CORINE Land Cover [WWW Document]. URL https://land.copernicus.eu/en/products/corine-land-cover (accessed 12.20.23).
Crowther, T.W., Todd-Brown, K.E.O., Rowe, C.W., Wieder, W.R., Carey, J.C., Machmuller, M.B., Snoek, B.L., Fang, S., Zhou, G., Allison, S.D., Blair, J.M., Bridgham, S.D., Burton, A.J., Carrillo, Y., Reich, P.B., Clark, J.S., Classen, A.T., Dijkstra, F.A., Elberling, B., Emmett, B.A., Estiarte, M., Frey, S.D., Guo, J., Harte, J., Jiang, L., Johnson, B.R., Kröel-Dulay, G., Larsen, K.S., Laudon, H., Lavallee, J.M., Luo, Y., Lupascu, M., Ma, L.N., Marhan, S., Michelsen, A., Mohan, J., Niu, S., Pendall, E., Peñuelas, J., Pfeifer-Meister, L., Poll, C., Reinsch, S., Reynolds, L.L., Schmidt, I.K., Sistla, S., Sokol, N.W., Templer, P.H., Treseder, K.K., Welker, J.M., Bradford, M.A., 2016. Quantifying global soil carbon losses in response to warming. Nature 540, 104–108. https://doi.org/10.1038/nature20150.
Dambrine, E., 1985. Contribution à l'étude de la répartition et du fonctionnement des sols de haute montagne : massifs des Aiguilles Rouges et du Mont-Blanc.
Davidson, E.A., Janssens, I.A., 2006. Temperature sensitivity of soil carbon decomposition and feedbacks to climate change. Nature 440, 165–173. https://doi.org/10.1038/nature04514.
De Reu, J., Bourgeois, J., Bats, M., Zwertvaegher, A., Gelorini, V., De Smedt, P., Chu, W., Antrop, M., De Maeyer, P., Finke, P., Van Meirvenne, M., Verniers, J., Crombé, P., 2013. Application of the topographic position index to heterogeneous landscapes. Geomorphology 186, 39–49. https://doi.org/10.1016/j.geomorph.2012.12.015.
Delahaie, A.A., Barré, P., Baudin, F., Arrouays, D., Bispo, A., Boulonne, L., Chenu, C., Jolivet, C., Martin, M.P., Ratié, C., Saby, N.P.A., Savignac, F., Cécillon, L., 2023. Elemental stoichiometry and Rock-Eval® thermal stability of organic matter in French topsoils. Soil 9, 209–229. https://doi.org/10.5194/soil-9-209-2023.
Delgado-Baquerizo, M., Eldridge, D.J., Maestre, F.T., Karunaratne, S.B., Trivedi, P., Reich, P.B., Singh, B.K., 2017. Climate legacies drive global soil carbon stocks in terrestrial ecosystems. Sci. Adv. 3.
Dinno, A., 2024. paran: Horn's Test of Principal Components/Factors - https://cran.r-project.org/web/packages/paran/index.html.
Disnar, J.R., Guillet, B., Keravis, D., Di-Giovanni, C., Sebag, D., 2003. Soil organic matter (SOM) characterization by Rock-Eval pyrolysis: scope and limitations. Org Geochem. 34, 327–343. https://doi.org/10.1016/S0146-6380(02)00239-5.
Djukic, I., Zehetner, F., Tatzber, M., Gerzabek, M.H., 2010. Soil organic-matter stocks and characteristics along an Alpine elevation gradient. J. Plant Nutr. Soil Sci. 173, 30–38. https://doi.org/10.1002/jpln.200900027.
Doetterl, S., Stevens, A., Six, J., Merckx, R., Van Oost, K., Casanova Pinto, M., Casanova-Katny, A., Muñoz, C., Boudin, M., Zagal Venegas, E., Boeckx, P., 2015. Soil carbon storage controlled by interactions between geochemistry and climate. Nat. Geosci. 8, 780–783. https://doi.org/10.1038/ngeo2516.
Dorrepaal, E., Toet, S., van Logtestijn, R.S.P., Swart, E., van de Weg, M.J., Callaghan, T. V., Aerts, R., 2009. Carbon respiration from subsurface peat accelerated by climate warming in the subarctic. Nature 460, 616–619. https://doi.org/10.1038/nature08216.
Duchaufour, P., Faivre, P., Poulenard, J., Gury, M., 2024. Introduction à la science du sol, Dunod (8e édition). ed.
Durand, Y., Giraud, G., Laternser, M., Etchevers, P., Mérindol, L., Lesaffre, B., 2009. Reanalysis of 47 Years of climate in the French Alps (1958–2005): Climatology and Trends for Snow Cover. J. Appl. Meteorol. Climatol. 48, 2487–2512. https://doi.org/10.1175/2009JAMC1810.1.
EEA, E.E.A., 2024. European Climate Risk Assessment (Publication No. 01/2024).
Egli, M., Mirabella, A., Sartori, G., Zanelli, R., Bischof, S., 2006. Effect of north and south exposure on weathering rates and clay mineral formation in Alpine soils. Catena 67, 155–174. https://doi.org/10.1016/j.catena.2006.02.010.
Egli, M., Poulenard, J., 2016. Soils of Mountainous Landscapes, in: International Encyclopedia of Geography. John Wiley & Sons, Ltd, pp. 1–10. https://doi.org/10.1002/9781118786352.wbieg0197.
Egli, M., Sartori, G., Mirabella, A., Favilli, F., Giaccai, D., Delbos, E., 2009. Effect of north and south exposure on organic matter in high Alpine soils. Geoderma 149, 124–136. https://doi.org/10.1016/j.geoderma.2008.11.027.
FAO, Jahn, R., Blume, H.P., Asio, V.B., Spaargaren, O., Schad, P., 2006. Guidelines for soil description, 4th edition. FAO, Rome.
Garcia-Pausas, J., Casals, P., Camarero, L., Huguet, C., Sebastià, M.-T., Thompson, R., Romanyà, J., 2007. Soil Organic Carbon Storage in Mountain Grasslands of the Pyrenees: Effects of climate and Topography. Biogeochemistry 82, 279–289.
Goldschmidt, V.M., 1930. Geochemische Verteilungsgesetze und kosmische Häufigkeit der Elemente. Naturwissenschaften 18, 999–1013. https://doi.org/10.1007/BF01492200.
Guidi, C., Vesterdal, L., Gianelle, D., Rodeghiero, M., 2014. Changes in soil organic carbon and nitrogen following forest expansion on grassland in the Southern Alps. For. Ecol. Manag. 328, 103–116. https://doi.org/10.1016/j.foreco.2014.05.025.
Heckman, K., Welty-Bernard, A., Rasmussen, C., Schwartz, E., 2009. Geologic controls of soil carbon cycling and microbial dynamics in temperate conifer forests. Chem. Geol. 267, 12–23. https://doi.org/10.1016/j.chemgeo.2009.01.004.
Hengl, T., de Jesus, J.M., Heuvelink, G.B.M., Gonzalez, M.R., Kilibarda, M., Blagotić, A., Shangguan, W., Wright, M.N., Geng, X., Bauer-Marschallinger, B., Guevara, M.A., Vargas, R., MacMillan, R.A., Batjes, N.H., Leenaars, J.G.B., Ribeiro, E., Wheeler, I., Mantel, S., Kempen, B., 2017. SoilGrids250m: Global gridded soil information based on machine learning. PLoS One 12, e0169748. https://doi.org/10.1371/journal.pone.0169748.
Hijmans, R.J., Bivand, R., Pebesma, E., Sumner, M.D., 2023a. terra: Spatial Data Analysis.
Hijmans, R.J., Etten, J. van, Sumner, M., Cheng, J., Baston, D., Bevan, A., Bivand, R., Busetto, L., Canty, M., Fasoli, B., Forrest, D., Ghosh, A., Golicher, D., Gray, J., Greenberg, J.A., Hiemstra, P., Hingee, K., Ilich, A., Geosciences, I. for M.A., Karney, C., Mattiuzzi, M., Mosher, S., Naimi, B., Nowosad, J., Pebesma, E., Lamigueiro, O.P., Racine, E.B., Rowlingson, B., Shortridge, A., Venables, B., Wueest, R., 2023b. raster: Geographic Data Analysis and Modeling.
IGN, 2001. BD ALTI® | Géoservices [WWW Document]. URL https://geoservices.ign.fr/bdalti (accessed 12.19.23).
Jenny, H., 1947. Factors of soil formation: a system of quantitative pedology. Dover, New York.
Jobbagy, E.G., Jackson, R.B., 2000. THE VERTICAL DISTRIBUTION OF SOIL ORGANIC CARBON AND ITS RELATION TO CLIMATE AND VEGETATION. Ecol. Appl. 10.
John, B., Yamashita, T., Ludwig, B., Flessa, H., 2005. Storage of organic carbon in aggregate and density fractions of silty soils under different types of land use. Geoderma, Mechanisms and Regulation of Organic Matter Stabilisation in Soils 128, 63–79. https://doi.org/10.1016/j.geoderma.2004.12.013.
Jonasson, S., 1988. Evaluation of the Point Intercept Method for the Estimation of Plant Biomass. Oikos 52, 101–106. https://doi.org/10.2307/3565988.
Kanari, E., Barré, P., Baudin, F., Berthelot, A., Bouton, N., Gosselin, F., Soucémarianadin, L., Savignac, F., Cécillon, L., 2021. Predicting Rock-Eval® thermal analysis parameters of a soil layer based on samples from its sublayers; an experimental study on forest soils. Org Geochem. 160, 104289. https://doi.org/10.1016/j.orggeochem.2021.104289.
Kemppinen, J., Lembrechts, J.J., Van Meerbeek, K., Carnicer, J., Chardon, N.I., Kardol, P., Lenoir, J., Liu, D., Maclean, I., Pergl, J., Saccone, P., Senior, R.A., Shen, T., Słowińska, S., Vandvik, V., von Oppen, J., Aalto, J., Ayalew, B., Bates, O., Bertelsmeier, C., Bertrand, R., Beugnon, R., Borderieux, J., Brůna, J., Buckley, L., Bujan, J., Casanova-Katny, A., Christiansen, D.M., Collart, F., De Lombaerde, E., De Pauw, K., Depauw, L., Di Musciano, M., Díaz Borrego, R., Díaz-Calafat, J., Ellis-Soto, D., Esteban, R., de Jong, G.F., Gallois, E., Garcia, M.B., Gillerot, L., Greiser, C., Gril, E., Haesen, S., Hampe, A., Hedwall, P.-O., Hes, G., Hespanhol, H., Hoffrén, R., Hylander, K., Jiménez-Alfaro, B., Jucker, T., Klinges, D., Kolstela, J., Kopecký, M., Kovács, B., Maeda, E.E., Máliš, F., Man, M., Mathiak, C., Meineri, E., Naujokaitis-Lewis, I., Nijs, I., Normand, S., Nuñez, M., Orczewska, A., Peña-Aguilera, P.,

Pincebourde, S., Plichta, R., Quick, S., Renault, D., Ricci, L., Rissanen, T., Segura-Hernández, L., Selvi, F., Serra-Diaz, J.M., Soifer, L., Spicher, F., Svenning, J.-C., Tamian, A., Thomaes, A., Thoonen, M., Trew, B., Van de Vondel, S., van den Brink, L., Vangansbeke, P., Verdonck, S., Vitkova, M., Vives-Ingla, M., von Schmalensee, L., Wang, R., Wild, J., Williamson, J., Zellweger, F., Zhou, X., Zuza, E. J., De Frenne, P., 2024. Microclimate, an important part of ecology and biogeography. Glob. Ecol. Biogeogr. 33, e13834. https://doi.org/10.1111/geb.13834.

Khedim, N., Cécillon, L., Poulenard, J., Barré, P., Baudin, F., Marta, S., Rabatel, A., Dentant, C., Cauvy-Fraunié, S., Anthelme, F., Gielly, L., Ambrosini, R., Franzetti, A., Azzoni, R.S., Caccianiga, M.S., Compostella, C., Clague, J., Tielidze, L., Messager, E., Choler, P., Ficetola, G.F., 2021. Topsoil organic matter build-up in glacier forelands around the world. Glob. Chang. Biol. 27, 1662–1677. https://doi.org/10.1111/gcb.15496.

Kögel-Knabner, I., Guggenberger, G., Kleber, M., Kandeler, E., Kalbitz, K., Scheu, S., Eusterhues, K., Leinweber, P., 2008. Organo-mineral associations in temperate soils: Integrating biology, mineralogy, and organic matter chemistry. J. Plant Nutr. Soil Sci. 171, 61–82. https://doi.org/10.1002/jpln.200700048.

Körner, C., 2003. Alpine plant life, 2nd Edt. ed. Springer, Heidelberg.

Körner, C., Paulsen, J., 2004. A world-wide study of high altitude treeline temperatures. J. Biogeogr. 31, 713–732. https://doi.org/10.1111/j.1365-2699.2003.01043.x.

Krettek, A., Herrmann, L., Rennert, T., 2020. Podzolisation affects the spatial allocation and chemical composition of soil organic matter fractions. Soil Res. 58, 713. https://doi.org/10.1071/SR20164.

Laliberté, E., Grace, J.B., Huston, M.A., Lambers, H., Teste, F.P., Turner, B.L., Wardle, D. A., 2013. How does pedogenesis drive plant diversity? Trends Ecol. Evol 28, 331–340. https://doi.org/10.1016/j.tree.2013.02.008.

Lefcheck, J., Byrnes, J., Grace, J., 2023. piecewiseSEM: Piecewise Structural Equation Modeling.

Legros, J.-P., 2007. Facteurs de la pédogénèse - Chapitre 2. Les Grands Sols Du Monde. 29–93.

Leifeld, J., Bassin, S., Fuhrer, J., 2005. Carbon stocks in swiss agricultural soils predicted by land-use, soil characteristics, and altitude. Agric. Ecosyst. Environ. 105, 255–266. https://doi.org/10.1016/j.agee.2004.03.006.

Leifeld, J., Zimmermann, M., Fuhrer, J., Conen, F., 2009. Storage and turnover of carbon in grassland soils along an elevation gradient in the Swiss Alps. Glob. Chang. Biol. 15, 668–679. https://doi.org/10.1111/j.1365-2486.2008.01782.x.

Liao, J.X., Liang, D.Y., Jiang, Q.W., Mo, L., Pu, G.Z., Zhang, D., 2020. Growth performance and element concentrations reveal the calcicole-calcifuge behavior of three Adiantum species. BMC Plant Biol. 20, 327. https://doi.org/10.1186/s12870-020-02538-6.

Lorenz, K., Lal, R., Preston, C.M., Nierop, K.G.J., 2007. Strengthening the soil organic carbon pool by increasing contributions from recalcitrant aliphatic bio(macro) molecules. Geoderma 142, 1–10. https://doi.org/10.1016/j.geoderma.2007.07.013.

Martinez-Almoyna, C., Saillard, A., Zinger, L., Lionnet, C., Arnoldi, C., Foulquier, A., Gielly, L., Piton, G., Münkemüller, T., Thuiller, W., 2022. Differential effects of soil trophic networks on microbial decomposition activity in mountain ecosystems. Soil Biol. Biochem. 172, 108771. https://doi.org/10.1016/j.soilbio.2022.108771.

Meng, Z., Mengxu, Z., Liu, W., Deo, R., Zhang, C., Yang, L., 2019. Soil organic carbon in semiarid alpine regions: the spatial distribution, stock estimation, and environmental controls. J. Soil. Sediment. https://doi.org/10.1007/s11368-019-02295-6.

Mulder, V.L., Lacoste, M., Richer-de-Forges, A.C., Martin, M.P., Arrouays, D., 2016. National versus global modelling the 3D distribution of soil organic carbon in mainland France. Geoderma 263, 16–34. https://doi.org/10.1016/j.geoderma.2015.08.035.

Murphy, M.V., 2022. semEff: Automatic Calculation of Effects for Piecewise Structural Equation Models.

NF ISO 10390 [WWW Document], n.d. . Afnor Ed. URL https://www.boutique.afnor.org/fr-fr/norme/nf-iso-10390/qualite-du-sol-determination-du-ph/fa117123/25226 (accessed 4.16.25).

Oksanen, J., Simpson, G.L., Blanchet, F.G., Kindt, R., Legendre, P., Minchin, P.R., O'Hara, R.B., Solymos, P., Stevens, M.H.H., Szoecs, E., Wagner, H., Barbour, M., Bedward, M., Bolker, B., Borcard, D., Carvalho, G., Chirico, M., Caceres, M.D., Durand, S., Evangelista, H.B.A., FitzJohn, R., Friendly, M., Furneaux, B., Hannigan, G., Hill, M.O., Lahti, L., McGlinn, D., Ouellette, M.-H., Cunha, E.R., Smith, T., Stier, A., Braak, C.J.F.T., Weedon, J., 2022. vegan: Community Ecology Package.

Pan, Y., Ren, L., Huo, J., Xiang, X., Meng, D., Wang, Y., Yu, C., Liu, Y., Suo, J., Huang, Y., 2024. Soil geochemistry prevails over root functional traits in controlling soil organic carbon fractions of the alpine meadow on the Qinghai-Tibet Plateau, China. CATENA 237, 107814. https://doi.org/10.1016/j.catena.2024.107814.

Patton, N.R., Lohse, K.A., Seyfried, M.S., Godsey, S.E., Parsons, S.B., 2019. Topographic controls of soil organic carbon on soil-mantled landscapes. Sci. Rep. 9, 6390. https://doi.org/10.1038/s41598-019-42556-5.

Pebesma, E., Bivand, R., Racine, E., Sumner, M., Cook, I., Keitt, T., Lovelace, R., Wickham, H., Ooms, J., Müller, K., Pedersen, T.L., Baston, D., Dunnington, D., 2023. sf: Simple Features for R.

Pepin, N., Bradley, R.S., Diaz, H.F., Baraer, M., Caceres, E.B., Forsythe, N., Fowler, H., Greenwood, G., Hashmi, M.Z., Liu, X.D., Miller, J.R., Ning, L., Ohmura, A., Palazzi, E., Rangwala, I., Schöner, W., Severskiy, I., Shahgedanova, M., Wang, M.B., Williamson, S.N., Yang, D.Q., Mountain Research Initiative EDW Working Group, 2015. Elevation-dependent warming in mountain regions of the world. Nat. Clim. Change 5, 424–430. https://doi.org/10.1038/nclimate2563.

Poeplau, C., Vos, C., Don, A., 2017. Soil organic carbon stocks are systematically overestimated by misuse of the parameters bulk density and rock fragment content. Soil 3, 61–66. https://doi.org/10.5194/soil-3-61-2017.

Prietzel, J., Zimmermann, L., Schubert, A., Christophel, D., 2016. Organic matter losses in German Alps forest soils since the 1970s most likely caused by warming. Nat. Geosci. 9, 543–548. https://doi.org/10.1038/ngeo2732.

Puissant, J., Briony, J., Goodall, T., Mang, D., Blaud, A., Gweon, H.S., Malik, A., Jones, D. L., Clark, I.M., Hirsch, P.R., Griffiths, R., 2019. The pH optimum of soil exoenzymes adapt to long term changes in soil pH. Soil Biol. Biochem. 138, 107601. https://doi.org/10.1016/j.soilbio.2019.107601.

R Core Team, 2023. R: A Language and Environment for Statistical Computing. R Found. Stat. Comput. https://www.R-project.org/.

RMQS, 2017. La carte nationale des stocks de carbone des sols intégrée dans la carte mondiale de la FAO - Martin Manuel - GIS Sol. https://doi.org/10.15454/JCONRJ.

Rowley, M.C., Grand, S., Verrecchia, É.P., 2018. Calcium-mediated stabilisation of soil organic carbon. Biogeochemistry 137, 27–49. https://doi.org/10.1007/s10533-017-0410-1.

Saenger, A., Cécillon, L., Poulenard, J., Bureau, F., De Daniéli, S., Gonzalez, J.-M., Brun, J.-J., 2015. Surveying the carbon pools of mountain soils: a comparison of physical fractionation and Rock-Eval pyrolysis. Geoderma 241–242, 279–288. https://doi.org/10.1016/j.geoderma.2014.12.001.

Schadt, C.W., Martin, A.P., Lipson, D.A., Schmidt, S.K., 2003. Seasonal Dynamics of previously unknown Fungal Lineages in Tundra Soils. Science 301, 1359–1361. https://doi.org/10.1126/science.1086940.

Schmidt, M.W.I., Torn, M.S., Abiven, S., Dittmar, T., Guggenberger, G., Janssens, I.A., Kleber, M., Kögel-Knabner, I., Lehmann, J., Manning, D.A.C., Nannipieri, P., Rasse, D.P., Weiner, S., Trumbore, S.E., 2011. Persistence of soil organic matter as an ecosystem property. Nature 478, 49–56. https://doi.org/10.1038/nature10386.

Schulze, K., Borken, W., Muhr, J., Matzner, E., 2009. Stock, turnover time and accumulation of organic matter in bulk and density fractions of a Podzol soil. Eur. J. Soil Sci. 60, 567–577. https://doi.org/10.1111/j.1365-2389.2009.01134.x.

Sebag, D., Verrecchia, E.P., Cécillon, L., Adatte, T., Albrecht, R., Aubert, M., Bureau, F., Cailleau, G., Copard, Y., Decaens, T., Disnar, J.-R., Hetényi, M., Nyilas, T., Trombino, L., 2016. Dynamics of soil organic matter based on new Rock-Eval indices. Geoderma 284, 185–203. https://doi.org/10.1016/j.geoderma.2016.08.025.

Shipley, B., 2000. A New Inferential Test for Path Models based on Directed Acyclic Graphs. Struct. Equ. Model. Multidiscip. J. 7, 206–218. https://doi.org/10.1207/S15328007SEM0702_4.

Sjögersten, S., Alewell, C., Cécillon, L., Hagedorn, F., Jandl, R., Leifeld, J., Martinsen, V., Schindlbacher, A., Sebastià, M.-T., Van Miegroet, H., 2011. Mountain Soils in a changing climate – Vulnerability of Carbon stocks and Ecosystem Feedbacks. In: Soil Carbon in Sensitive European Ecosystems. John Wiley & Sons Ltd, pp. 118–148. https://doi.org/10.1002/9781119970255.ch6.

Soucémarianadin, L., Cécillon, L., Chenu, C., Baudin, F., Nicolas, M., Girardin, C., Delahaie, A., Barré, P., 2019. Heterogeneity of the chemical composition and thermal stability of particulate organic matter in French forest soils. Geoderma 342, 65–74. https://doi.org/10.1016/j.geoderma.2019.02.008.

Stoner, S.W., Schrumpf, M., Hoyt, A., Sierra, C.A., Doetterl, S., Galy, V., Trumbore, S., 2023. How well does ramped thermal oxidation quantify the age distribution of soil carbon? Assessing thermal stability of physically and chemically fractionated soil organic matter. Biogeosciences 20, 3151–3163. https://doi.org/10.5194/bg-20-3151-2023.

Thébault, A., Clément, J.-C., Ibanez, S., Roy, J., Geremia, R.A., Pérez, C.A., Buttler, A., Estienne, Y., Lavorel, S., 2014. Nitrogen limitation and microbial diversity at the treeline. Oikos 123, 729–740. https://doi.org/10.1111/j.1600-0706.2013.00860.x.

Thuiller, W., Saillard, A., Abdulhak, S., Augé, V., Birck, C., Bonet, R., Choler, P., Delestrade, A., Kunstler, G., Leccia, M.-F., Lienard, B., Poulenard, J., Valay, J.-G., Bayle, A., Bonfanti, N., Brousset, L., Bizard, L., Calderón-Sanou, I., Dentant, C., Desjonquères, C., Gielly, L., Guéguen, M., Guiter, F., Hedde, M., Hustache, E., Kedhim, N., Lapenu, P., Guillarme, N.L., Marchal, L., Mahieu, C., Martin, G., Martinez-Almoyna, C., Miele, V., Murienne, J., Paillet, Y., Rome, M., Renaud, J., 2024. ORCHAMP: an observation network for monitoring Biodiversity and Ecosystem Functioning across Space and Time in Mountainous Regions. Comptes Rendus Biol. - Académie Sci.

Towett, E.K., Shepherd, K.D., Cadisch, G., 2013. Quantification of total element concentrations in soils using total X-ray fluorescence spectroscopy (TXRF). Sci. Total Environ. 463–464, 374–388. https://doi.org/10.1016/j.scitotenv.2013.05.068.

Trumbore, S.E., 1993. Comparison of carbon dynamics in tropical and temperate soils using radiocarbon measurements. Glob. Biogeochem. Cycles 7, 275–290. https://doi.org/10.1029/93GB00468.

Trumbore, S.E., Czimczik, C.I., 2008. An Uncertain Future for Soil Carbon. Science 321, 1455–1456. https://doi.org/10.1126/science.1160232.

Van Den Boogaart, K.G., Tolosana-Delgado, R., 2008. "compositions": a unified R package to analyze compositional data. Comput. Geosci. 34, 320–338. https://doi.org/10.1016/j.cageo.2006.11.017.

Vernay, M., Lafaysse, M., Monteiro, D., Hagenmuller, P., Nheili, R., Samacoïts, R., Verfaillie, D., Morin, S., 2022. The S2M meteorological and snow cover reanalysis over the French mountainous areas: description and evaluation (1958–2021). Earth Syst. Sci. Data 14, 1707–1733. https://doi.org/10.5194/essd-14-1707-2022.

Vionnet, V., Brun, E., Morin, S., Boone, A., Faroux, S., Le Moigne, P., Martin, E., Willemet, J.-M., 2012. The detailed snowpack scheme Crocus and its implementation in SURFEX v7.2. Geosci. Model Dev. 5, 773–791. https://doi.org/10.5194/gmd-5-773-2012.

Virto, I., Moni, C., Swanston, C., Chenu, C., 2010. Turnover of intra- and extra-aggregate organic matter at the silt-size scale. Geoderma 156, 1–10. https://doi.org/10.1016/j.geoderma.2009.12.028.

Vitousek, P., Farrington, H., 1997. Nutrient limitation and soil development: Experimental test of a biogeochemical theory. Biogeochemistry 37, 63–75. https://doi.org/10.1023/A:1005757218475.

Wadoux, A.M.J.-C., Malone, B., Minasny, B., Fajardo, M., McBratney, A.B., 2021. Soil Spectral Inference with R: Analysing Digital Soil Spectra using the R Programming Environment, Progress in Soil Science. Springer International Publishing, Cham. https://doi.org/10.1007/978-3-030-64896-1.

Wickham, H., Averick, M., Bryan, J., Chang, W., McGowan, L., François, R., Grolemund, G., Hayes, A., Henry, L., Hester, J., Kuhn, M., Pedersen, T., Miller, E., Bache, S., Müller, K., Ooms, J., Robinson, D., Seidel, D., Spinu, V., Takahashi, K., Vaughan, D., Wilke, C., Woo, K., Yutani, H., 2019. Welcome to the Tidyverse. J. Open Source Softw. 4, 1686. https://doi.org/10.21105/joss.01686.

Wiesmeier, M., Barthold, F., Spörlein, P., Geuß, U., Hangen, E., Reischl, A., Schilling, B., Angst, G., von Lützow, M., Kögel-Knabner, I., 2014. Estimation of total organic carbon storage and its driving factors in soils of Bavaria (southeast Germany). Geoderma Reg. 1, 67–78. https://doi.org/10.1016/j.geodrs.2014.09.001.

Wiesmeier, M., Urbanski, L., Hobley, E., Lang, B., von Lützow, M., Marin-Spiotta, E., van Wesemael, B., Rabot, E., Ließ, M., Garcia-Franco, N., Wollschläger, U., Vogel, H.-J., Kögel-Knabner, I., 2019. Soil organic carbon storage as a key function of soils - a review of drivers and indicators at various scales. Geoderma 333, 149–162. https://doi.org/10.1016/j.geoderma.2018.07.026.

WRB, I.W.G., 2022. World Reference Base for Soil Resources. International soil classification system for naming soils and creating legends for soil maps. 4th edition. International Union of Soil Sciences (IUSS), Vienna, Austria.

Xu, M., Li, X., Cai, X., Gai, J., Li, X., Christie, P., Zhang, J., 2014. Soil microbial community structure and activity along a montane elevational gradient on the Tibetan Plateau. Eur. J. Soil Biol. 64, 6–14. https://doi.org/10.1016/j.ejsobi.2014.06.002.

Yang, S., Jansen, B., Kalbitz, K., Chunga Castro, F.O., van Hall, R.L., Cammeraat, E.L.H., 2020. Lithology controlled soil organic carbon stabilization in an alpine grassland of the Peruvian Andes. Environ. Earth Sci. 79, 66. https://doi.org/10.1007/s12665-019-8796-9.

Yang, Y., Halbritter, A.H., Klanderud, K., Telford, R.J., Wang, G., Vandvik, V., 2018. Transplants, Open Top Chambers (OTCs) and Gradient Studies ask different questions in climate Change Effects Studies. Front. Plant Sci. 9. https://doi.org/10.3389/fpls.2018.01574.

Zhang, F., Li, H., Zhu, J., Si, M., Fan, B., Zhou, H., Li, Y., 2025. Precipitation Determines the Spatial Variability of Vegetation and Topsoil Organic Carbon Densities of Alpine Grasslands in the Qinghai-Tibetan Plateau, China. Ecosystems 28, 12. https://doi.org/10.1007/s10021-024-00957-2.

Zhongsheng, Z., Shan, J., Wenwen, Z., Qiang, G., Haitao, W., 2023. Which is more important in stabilizing soil organic carbon in mountain ecosystems: molecular features, mineral protection, soil nutrients, or elevation? Catena 232, 107395. https://doi.org/10.1016/j.catena.2023.107395.